THESIS PAPER

ON

EXTERIOR AND INTERIOR ACOUSTIC ANALYSIS OF RIGID CAVITY

Submitted by

DIBYAYATI SAHANA
MASTER OF CIVIL ENGINEERING
(STRUCTURAL ENGINEERING)
2ND Year (2018-2019)
Roll No - MCE001710402008
Exam Roll No -M4CIV19013
Registration No – 140635 of 2017-2018

In partial fulfilment of the requirement for the degree of

M.E.
in

CIVIL ENGINEERING
(Specialisation- STRUCTURAL ENGINEERING)

under the guidance of

Dr. SREYASHI DAS (PAL)

DEPARTMENT OF CIVIL ENGINEERING

FACULTY OF ENGINEERING AND TECHNOLOGY

JADAVPUR UNIVERSITY

JADAVPUR UNIVERSITY

FACULTY OF ENGINEERING AND TECHNOLOGY

DEPARTMENT OF CIVIL ENGINEERING

JADAVPUR, KOLKATA-700032

CERTIFICATE OF RECOMMENDATION

This is to certify that DIBYAYATI SAHANA (Exam Roll No M4CIV19013, Registration no 140635 of 2017-2018) has carried out the thesis work entitled "**EXTERIOR AND INTERIOR ACOUSTIC ANALYSIS OF RIGID CAVITY"** under my direct supervision & guidance. She carried out this work independently. I hereby recommend that the thesis be accepted in partial fulfillment of the requirements for awarding the degree of "**MASTER OF ENGINEERING IN CIVIL ENGINEERING (STRUCTURAL ENGINEERING**)".

Countersigned by

……………………………………………………………………………

Assistant Professor (Dr.) Sreyashi Das (Pal)
Department of civil engineering
Jadavpur University
Kolkata- 700 032

……………………………………………

DEAN
Prof. Chiranjib Bhattacharjee
Faculty of Engineering and Technology
Jadavpur University
Kolkata- 700 032

………………………………………………………

(H.O.D)
Prof. Dipankar Chakravorty
Department of civil engineering
Jadavpur University
Kolkata- 700 032

JADAVPUR UNIVERSITY

FACULTY OF ENGINEERING AND TECHNOLOGY

DEPARTMENT OF CIVIL ENGINEERING

JADAVPUR, KOLKATA-700032

CERTIFICATE OF APPROVAL

This foregoing thesis is hereby approved as credible study on an Engineering Subject carried out and presented in a manner satisfactory to warrant its acceptance as a prerequisite to the degree for which it has been submitted.

Committee of final examination

For evaluation of the thesis.

....

Signature of examiner

………………………………………

Signature of examiner

DECLARATION

I, Dibyayati Sahana a student of Master of engineering in civil engineering dept. (structural engineering), Jadavpur university, Faculty of engineering & technology, hereby declare that the work being presented in the thesis work entitled, **"Exterior and Interior Acoustic Analysis of Rigid Cavity"** is authentic record of work that has been carried out at the Department of civil engineering**,** Jadavpur university, under Assistant Professor Dr. Sreyashi Pal Department of civil engineering**,** Jadavpur university.

The work contained in the thesis has not yet been submitted in part or full to any other university or institution or professional body for award of any degree or diploma or any fellowship.

Date: (Dibyayati Sahana)

Place: Jadavpur Exam Roll No- M4CIV19013

Reg No- 140635 of 2017-18

ACKNOWLEDGEMENTS

First of all, I would like to express my gratitude to my supervisor, Assistant Professor (Dr.) Sreyashi Das (Pal), for her valuable contributions and advice through the course of my post graduate studies. Her guidance and support are the main reasons that made the completion of this research possible. Her patience and availability for any help whenever needed with her heavy workload is appreciated.

My sincere appreciation goes to my fellow post graduates. I am also thankful to other researchers of our department to clarify my doubt and others technical assistance.

Finally, I would like to thank my family and my all friends, for their constant encouragement during the difficult times, of my family.

Date: ……………………………………………….

Place: Jadavpur Dibyayati Sahana

Exam Roll No- M4CIV19013

Reg No- 140635 of 2017-18

CONTENTS

LIST OF FIGURES

1. INTRODUCTION

1.1 ACOUSTIC ANALYSIS: INTERIOR AND EXTERIOR

Acoustics is the branch of physics that deals with the study of all mechanical waves in gases, liquids, and solids including topics such as vibration, sound, ultrasound and infrasound. The study of acoustics revolves around the generation, propagation and reception of mechanical waves and vibrations. There are many kinds of cause, both natural and volitional. There are many kinds of transduction process that convert energy from some other form into sonic energy, producing a sound wave. There is one fundamental equation that describes sound wave propagation, the acoustic wave equation, but the phenomenon that emerge from it are varied and often complex. The wave carries energy throughout the propagating medium. Eventually this energy is transduced again into other forms, in ways that again may be natural or volitionally contrived. The central stage in the acoustical process is wave propagation. This falls within the domain of physical acoustics. In fluids, sound propagates primarily as a pressure wave. In solids, mechanical waves can take many forms including longitudinal waves, transverse waves and surface waves. Acoustics looks first at the pressure levels and frequencies in the sound wave and how the wave interacts with the environment. While propagation, disturbances is related to the sound pressure level (SPL) which is measured on a logarithmic scale in decibels.

Excessive exposure to high sound pressure level (SPL) causes hearing damage. It affects mental concentration and quality of work too. Hence good acoustic design is very important as it provides contentment and leads to a healthy life. Therefore prediction of the acoustic field due to arbitrarily shaped structures is an important research area in many disciplines. This topic has variety of applications especially, in engineering and automotive engineering fields in determining the interior noise levels of aircraft and ground vehicles. In the past, a great deal of effort has been put into studying methods of reducing high frequency noise inside the cabins of aircraft. Researches are carried out to reduce the noise to acceptable levels from the point of view of passenger comfort, by means of careful design and vibration isolation techniques.

Exterior acoustic analysis is required mostly for strategic reasons and avoiding community noise pollution problems whereas interior acoustic analysis is mainly needed for human comfort and health as well as structural safety, integrity and economy.

Insight into the behaviour of many practical sound sources, such as vibrating surfaces, jet flows, and combustion, can be obtained by considering elementary sources. It begins by discussing sources that are so small in comparison with the wavelength of the sound they produce that the sources can be considered as concentrated at a single point. The simplest source to deal with mathematically is a vanishingly small pulsating sphere with a finite volume velocity. Such a source is called a monopole, a point source or a simple source. Any source that changes its volume as a function of time may be approximated by a monopole source at frequencies where it is small compared with the wavelength.

The different forms of the sound field radiated from different surfaces at low and at high frequencies provide physical insight into practical acoustic sources involving vibrating surfaces, such as loud speakers and active sonar systems. Also estimate of far field sound pressure level is important for a vibrating structure radiating sound.

For the solution of these problems several methods have been used so far, use of the finite element method, statistical energy analysis, and boundary element method (BEM) with integral formulations being the most prominent. Each method has its advantage and drawbacks depending on the particular application in hand.

1.2 BOUNDARY ELEMENT METHOD

The boundary element method (BEM) constitutes a technique for analysing the behaviour of mechanical systems and especially of engineering structures subjected to external loading. The term loading is used here in the general sense, referring to the external source which produces a non-zero field function that describes the response of the system (temperature field, displacement field, stress field, etc.), and it may be heat, surface tractions, body forces, or even non-homogeneous boundary conditions, e.g. support settlement. Today the BEM is being applied to all fields of engineering such as the potential theory, acoustics, torsion, electric and magnetic field theory, elastostatics, elastodynamics, plate and shell analysis, transient heat transfer, viscoelasticity, viscoplasticity, fracture mechanics, water waves, viscous fluid flow, ground water flow and thermoelasticity, etc. The method is even used to investigate into the micro-mechanical behaviour of the fibre reinforced composite materials.

In principle, the method is based on finding the unknown solutions at the boundary in light of a second set of known boundary solution, derived from the Green's solution of the governing equation, the two solutions being connected through Gauss Divergence theorem, for a set of given boundary conditions. The boundary conditions are incorporated into the system equation before going for the solution. Any solution that is needed inside the domain can be calculated from the boundary solutions, once the boundary values are known.

1.3 BOUNARY ELEMENT METHOD (BEM) OVER FINITE ELEMENT METHOD (FEM)

There are certain advantages of BEM over FEM. Modelling with finite elements can be ineffective and laborious for certain classes of problems, is not free of drawbacks. The most important reasons are:

I. Discretization is over the entire domain occupied by the body. Hence, generation and inspection of the finite element mesh exhibit difficulty and are both laborious and time consuming, especially when the geometry of the body is not simple. For example, when there are holes, notches or corners, mesh refinement and high element density is required at these critical regions of large solution gradients.

II. Modification of the discretized model to improve the accuracy of the solution or to reflect design changes can be difficult and requires a lot of effort and time.

III. For infinite domains, e.g. half space or the complementary domain to a finite one, fabrication or fictitious closed boundaries is required in order to apply the FEM. This reduces the accuracy and some time may result in spurious or incorrect solutions.

IV. For problems described by differential equations of fourth or higher order (i.e., plate equations, or shell equations of sixth, eighth or higher order), the conformity requirements demand such a tedious job that FEM may become impractical.

On the contrary, the boundary element method possesses many advantages, the most important of which are:

I. Discretization is only over the boundary of the body, making numerical modelling with the BEM easy and reducing the number of unknowns by one order. Thus, a remodelling to reflect design changes becomes simple.

II. For infinite domains, the problem is formulated simply as an exterior one, apparently, the fundamental solution has to satisfy some conditions at infinity, such as sommerfeld's radiation condition for problems in acoustics. In this manner, computer programs developed for finite domains can be used, with just few modifications, to solve problems in infinite domains. This is not possible with the FEM.

III. The method is particularly effective in computing the derivatives of the field function (e.g., fluxes, strains, stresses, moments). It can easily handle concentrated forces and moments, either inside the domain or on the boundary.

IV. The BEM allows evaluation of the solution and its derivatives at any point of the domain of the problem and at any instant in time. This is feasible because the method uses an integral representation of the solution as a continuous mathematical expression, which can be differentiated and utilized as a mathematical formula. This is impossible with the FEM, since the solution is obtained only at the nodal points.

V. The method is well suited for solving problems in domains with geometric peculiarities, such as cracks.

1.4 NEED OF BOUNDARY ELEMENT METHOD FOR ACOUSTIC ANALYSIS

Over recent decades, the boundary element method (BEM) has received much attention from researchers and has become an important technique in the computational solution of a number of physical problems. In common with the better known finite element method (FEM) and finite difference method (FDM), the boundary element method is essentially a method for solving partial differential equations (PDEs) and can only be employed when the physical problem can be expressed as such. As with the other methods mentioned, the boundary element method is a numerical method and hence it is an important subject of research amongst the numerical analysis community. The boundary element method has found application in such diverse topics as stress analysis, potential flow, fracture mechanics and acoustics.

Acoustics is an important branch of physical science. An acoustic field can exist in a fluid domain such as air or water, the two most important acoustic media. The linear wave equation forms an acceptable model in many fluids and it is often used in the cases of air and water media. In many physical situations the acoustic field is periodic, and has the outcome of reducing wave equation to a sequence of Helmholtz equations by a Fourier decomposition with one Helmholtz equation for each sample frequency. Solutions of acoustic problems are obtained through the consideration of the individual Helmholtz problems.

The Helmholtz equation governing a range of classes of domains may be solved by the boundary element method. Hence the BEM has received attention from engineers that are interested in applications such as the sound output of a loudspeaker, the noise from a radiating source such as an engine and the interior acoustic modes of an enclosure such as a vehicle interior. The method is equally applicable in underwater acoustics and can be used to model the scattering effect of an obstruction in the ocean or to determine the acoustic field surrounding a sonar transducer.

The advantage in the boundary element method arises from the fact that only the boundary of the domain of the PDE requires sub-division. Thus the dimension of the problem is effectively reduced by one, for example an equation governing a three dimensional region is transformed into one over its surface. In cases where the domain is exterior to the boundary, as it is in acoustic radiation and scattering models, the extent of the domain is infinite and hence the advantages of the BEM are even more striking; the equation governing the infinite domain is reduced to an equation over the finite boundary.

1.5 SCOPE OF THE WORK IN EXTERIOR AND INTERIOR ACOUSTICS

The present study involves analysis of exterior and interior acoustic analysis using BEM in two parts.

In the first part exterior acoustic analysis is shown. The acoustic radiation problem is emphasized because many noise control problems can be adequately modelled by assuming that the noise source is submerged in an infinite fluid medium. At low frequencies where the acoustic wavelength is much larger that the characteristic dimension of the vibrating structure, the acoustic radiation can be modelled as equivalent to that of a simple point source. Analysis of sound pressure level for pulsating sphere and other arbitrary structures i.e., a cube and a cylinder whose lateral surface is pulsating are shown. Sound pressure level (SPL) of the exterior domain has been plotted showing different patterns for different point sources. One of major problem regarding exterior acoustic is that of its non-uniqueness problem which has been taken care of by applying Combined Helmholtz Integral Equation Formulation (CHIEF) method. One CHIEF point has been used for the above simple sources which have proven to be helpful in removing irregularity for certain frequencies.

In the second part, interior acoustic analysis of rigid arbitrary shaped cavity have been shown having different shapes. Absorbent layer has been used in the interior cavity as a boundary condition to reduce the sound pressure level (SPL) at certain frequencies. Different case studies have been done regarding the shape and size of different cavity. The boundary as well as domain SPL has been determined by using boundary element method (BEM) with the help of MATLAB programming. It was shown that different position of absorbent layer behaves differently in reducing the SPL at a particular location and at specific frequency.

2. LITERATURE REVIEW

2.1 HISTORICAL DEVELOPMENT OF BOUNDARY ELEMENT METHOD

Until the beginning of the eighties, the BEM was known as Boundary Integral Equation Method (BIEM). As a method for solving problems of mathematical physics has its origin in the work of G. Green [1]. He formulated, in 1828, the integral representation of the solution for the Dirichlet and Neumann problems of Laplace equation by introducing the so-called Green's function for these problem. In 1872, Betti [2] presented a general method for integrating the equations of elasticity and deriving their solution in integral form. Basically, this may be regarded as a direct extension of Green's approach to the Navier equations of elasticity. In 1885, Somigliana [3] used Betti's reciprocal theorem to derive the integral representation of the solution of the elasticity problem, including its expression of the body forces, the boundary displacements and the tractions. Already in late eighties, one could find numerous publications in the literature, where the BEM was applied to a wide variety of engineering problems. Among them are static and dynamic, linear or non-linear problems of elasticity, of plates and shells, problems of elastodynamics, wave and earthquake engineering, geomechanics and foundation engineering, soil-structure interaction, fluid-structure interaction, fluid dynamics, unilateral contact, fracture mechanics, electricity and electromagnetism, heat conduction, acoustics, aerodynamics, corrosion, optimization, sensitivity analysis, inverse problems, problems of system identification, etc. it could be said that today the BEM has matured and become a powerful method for the analysis of engineering problems, and an alternative to the domain methods. The method has been established by the name BEM, which is attributed to the approach used to solve the boundary integral equations. Software based on the BEM has been developed for computers of simple or parallel architecture, along with professional high performance packages, like BEASY [4]. In 1978, C. Brebbia organized the first international conference on BEM, and since then conferences on BEM are organized yearly by the International Society for Boundary Elements (IABEM). Furthermore, all conferences on computational mechanics devote sessions to the BEM. The proceedings of the above conferences (BEM, IABEM) are referred to literature review articles [5,6].

2.2 BOUNDARY ELEMENT METHODS - NUMERICAL IMPLEMENTATION

One of the fundamental requirements for numerical modelling is a description of the problem, its boundaries, boundary conditions and material properties, in a mathematical way. The exact definition of the shape of a complicated boundary would require the specification of the location (relative to the origin set of axes) of a large number of points on the surface (indeed an exact definition will take an infinite number). In order to able to model such problems with a reasonable amount of input data, only a limited number of points may be defined and the shape between the points is approximated by functions. This is known as solid modelling [7]. Solid modelling is being used, for example, to describe the shape of car bodies in mechanical engineering and ore bodies in mining, for the purpose of generating displays on computer graphics terminals. Thus a new form of car body can be visualized, in perspective, from various angles, even before a scale model is built and the location and grade of ore bodies can be displayed for optimising excavation strategies in mine planning. Constant elements were used in the early days of the development, where the method was known under the name Boundary Integral Equation Method [8]. This is similar to the development of FEM, where triangular and tetrahedral elements, with exact integration, were used in the early days. In 1968, Ergatoudis and Irons [9] suggested that isoparametric finite elements and numerical integration could be used to obtain better results, with fewer elements. The concept of higher order elements and numerical integration is very appealing to engineers because it alleviates the need for tedious analytical integration and, more importantly, it allows the writing of general purpose software with a choice of element types. The idea of using isoparametric concepts for boundary elements seems to have been first introduced by Lachat and Watson [10] and this prompted a change of name of the method to Boundary Element Method.

2.3 EXTERIOR ACOUSTIC ANALYSIS

Classical formulations of acoustic radiation from vibrating bodies based on integral equations started in early 1960's. In these works, exterior steady-state acoustic radiation problem for bodies of arbitrary shape was investigated. Chen and Schwelkert [11] described the acoustic field by a distribution of surface sources of unknown strength at the shell-fluid boundaries, which led to a set of integral equations. This numerical technique is named as Simple Source Formulation (SSF) in which the acoustic pressure at an exterior field point is represented in terms of a surface integral of a source density function. Computational results were given for two sample problems such as a piston set in a rigid sphere, and a stiffened cylindrical shell of finite length in water. Chertock [12] developed a numerical method utilizing the discretized Surface Helmholtz Integral (SHIE) for the solution of radiation problems involving surfaces of revolution. Another approximate method was presented by Williams et al. [13] in which the farfield pressure was approximated by a truncated series of spherical Hankel functions. The method was shown to be most accurate for radiating surfaces that are nearly spherical in shape. Copley [14] proposed a method applicable to radiation from surfaces of revolution utilizing the Interior Helmholtz Integral Equation (IHIE). All three types of integral formulations for obtaining approximate solutions of the exterior steady-state acoustic radiation problem for an arbitrary surface were discussed by Schenck [15]. Schenck proposed a Combined Helmholtz Integral Formulation (CHIEF) to overcome the deficiencies and computational difficulties present in the previous works. He showed that this formulation yielded unique solutions even at the characteristic wave numbers for which the other integral equations broke down. Meyer, Bell, and Zinn [16] investigated the development of a procedure for the exterior sound radiation problems. They were concerned with the following points:

I. The development of a numerical scheme for handling the singular integrands encountered in the application of the Helmholtz formulae
II. The determination of the accuracy of the resulting solutions.

III. The determination of the most effective procedure for handling the non-uniqueness for the radiation solution at eigenvalues of the associated internal acoustic problem.

The Boundary Element Method (BEM) became popular in late 1970’s. koopman and Benner [17] presented a computational method based on Helmholtz integral for assessing the sound power characteristics of machines. The accuracy of the method was demonstrated by calculating the pressure on the surface of a uniformly pulsating sphere and of an oscillating sphere. A clear explanation of the application of the BEM to exterior sound radiation problems was given by Seybert et al [18]. The BEM was used to obtain numerical solutions to the same classical radiation problems. They introduced an isoparametric element formulation in which both the surface geometry and the acoustic variables on the surface of the radiating body were represented by quadratic shape functions. Solutions to the problems encountered in the use of BEM have been suggested by Piaszczyk [19] and Brod [20]. Recently, Wu et al [21] described a BEM code for acoustic analysis, along with the process of vectorizing and parallelizing the code on a vector parallel computer and Seybert, Cheng, and Wu presented an approach to the solution of coupled interior/exterior acoustic problems using the BEM [22].

2.4 INTERIOR ACOUSTIC ANALYSIS

The solution of the interior noise fields of cavities having arbitrary shapes by using BEM has recently received much interest. Bell, Meyer, and Zinn [23] presented an integral solution of the Helmholtz equation for predicting acoustic properties of arbitrarily shaped bodies. They examined two-dimensional problems of a circle and rectangle together with a duct having a right-angle bend. They also investigated the acoustic properties of a sphere using an axisymmetric formulation. A master plan for prediction of vehicle interior noise was suggested by Dowell [24]. The interior noise problem was presented considering noise sources, noise effects on people and payloads, noise reduction concepts, noise transmission analysis, and interior acoustic cavities. He examined the contributions to the literature on this subject and discussed the different methods of approach to the problem. Sestieri et al [25] discussed the structural-acoustic coupling problem by using the BEM for interior volumes having complex shapes. They investigated the importance of coupling and reached the conclusion that a full coupled analysis did not seem to be justified. Seybert and Cheng [26] concerned with the application of the BEM to interior acoustics problems governed by the reduced wave (Helmholtz) differential equation. They applied the BEM formulation to an axisymmetric problem at which the surface integrals could be reduced to line integrals along the generator of the cavity and to integrals over the angle of revolution. Therefore, the surface was discretized by using line elements, not surface elements and only the generator of the cavity needed to be discretized. They illustrated the solution for the acoustic response of a spherical cavity.

Fyfe [27] discussed the application of the BEM to predict the interior acoustic mode frequencies of an enclosed medium. He used a non-rectangular box and an automobile model to show the accuracy of the method. Cheng and Seybert [28] examined both the interior and exterior acoustic radiation problems considering the application of the BEM. The acoustical response of a spherical cavity was determined and good agreement between the BEM results and the analytical solution was obtained.

A more general investigation of the application of the BEM for the numerical solution of noise problems inside a complex shaped cavity was performed by Suzuki et al [29]. A new formulation for complicated boundary conditions was proposed to solve practical noise problems inside a vehicle cabin. The acoustic effect of absorbent materials on the vibrating surfaces and the effect of leakage through an opening were considered in the analysis. They applied the method in determining the sound pressure inside a linear duct, the transmission of sound through a cavity-backed plate, and predicting the sound pressure field inside a rather simple sedan compartment model. These studies resulted in the development of a new computer code called ACOUST/BOOM to analyse the sound pressure radiated by a vibrating structure and to calculate the acoustic resonance of the field [30]. In 2006, Niyogi [31] had analysed coupled structural acoustic problem using absorbent layer through admittance relations. In 2009, Han et al [32] predicted the absorption exponent in rectangular enclosures with a single absorbent boundary.

In this present study sound pressure level at the boundary and within the domain of an arbitrary shaped cavity have been found out. Boundary element analysis (BEA) has been used [33, 34, 35] to solve the acoustic cavity problem governed by wave equation, in frequency domain. Eight-noded isoparametric serendipity elements are used to model the boundary. A pressure-velocity formulation is adopted to model the acoustic domain. It was tried to control the sound pressure level using absorbent layer at different boundary.

3. THEORETICAL BACKGROUND

3.1 THEORETICAL FORMULATION

The boundary element formulation for the sonic response of exterior and interior acoustic domain is presented in this chapter. The governing acoustic equation (Helmholtz equation) is developed and the fundamental solution is presented and employed in conjunction with the Green's symmetric identity to generate the Helmholtz boundary integral equation (HBIE). The HBIE is the basis of a direct boundary element formulation for the acoustic response analysis. The present formulation adopts boundary pressure and normal fluid velocity at the nodes as the primary variables.

3.2 THE GOVERNING ACOUSTIC EQUATION

The equation of state for a gas relates the internal restoring forces to the corresponding deformations. Being very quick, the acoustic processes are nearly adiabatic, and so, their equation of state, assuming the medium to be a perfect gas, may be written as

$$\frac{P}{P_o} = \left(\frac{\rho}{\rho_o}\right)^{\gamma} \tag{3.2.1a}$$

where γ is the ratio of the specific heats of the gas at constant pressure to that at constant volume, P and P_o are the instantaneous and ambient pressures, respectively, and ρ and ρ_o are instantaneous and ambient mass densities, respectively, of the acoustic fluid. For the acoustic disturbances to be adiabatic there must not be any exchange of thermal energy between adjacent elements of fluid. Taylor's series expansion rule may now be applied to draw a relation between changes in pressure and density due to acoustic disturbances, as shown below

$$P = P_o + \left(\frac{\partial P}{\partial \rho}\right)_{\rho_o} (\rho - \rho_o) + \left(\frac{\partial^2 P}{\partial \rho^2}\right)_{\rho_o} (\rho - \rho_o)^2 / 2 + \cdots$$

where the partial derivatives are constants determined for the adiabatic compression and expansion of the fluid about its equilibrium density. Assuming the fluctuations are small, only the first order term in $(\rho-\rho_o)$ may be retained. This gives a linear relation between the pressure fluctuation and the change in density.

$$p = P - P_o = \left(\frac{\partial P}{\partial \rho}\right)_{\rho_o} (\rho-\rho_o) = B\frac{\rho-\rho_o}{\rho_o} = Bs \tag{3.2.1b}$$

where $B = \rho_o(\partial P/\partial\rho)_{\rho_o}$ is the adiabatic bulk modulus, and $s = (\rho-\rho_o)/\rho_o$ is the condensation. The numerical value of *s* is very small. In fact, for the intense sounds in air, which are painful to human ear, neither *s* nor the spatial rate of change of fluid particle displacement, $\partial\xi_{ai}/\partial x_j$, exceed the numerical value of 0.0001.

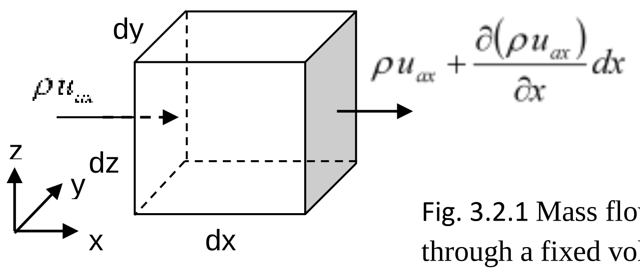

Fig. 3.2.1 Mass flow in the *x* direction through a fixed volume *dV*.

The equation of continuity for the acoustic fluid may be derived with reference to Fig. 3.2.1, exhibiting a fixed control volume *dV* = *dx dy dz* in space, through which fluid flows with velocity $\vec{u}_a$ ($\equiv \partial\xi_a/\partial t$) and instantaneous density ρ. The net influx of mass into this spatially fixed volume, resulting from flow in the *x* direction, is

$$-\frac{\partial(\rho u_{ax})}{\partial x}dV\,.$$

Similar expressions can be obtained for the *y* and *z* directions too, so that the total influx is

$$-\left[\frac{\partial(\rho u_{ax})}{\partial x}+\frac{\partial(\rho\, u_{ay})}{\partial y}+\frac{\partial(\rho\, u_{az})}{\partial z}\right]dV \equiv -\left[\nabla\cdot(\rho\vec{u}_a)\right]dV$$

where ∇ is the divergence operator. The rate with which the mass increases inside this volume is $(\partial\rho/\partial t)dV$. Since the net influx must equal the rate of increase, hence,

$$\frac{\partial\rho}{\partial t} + \nabla\cdot(\rho\vec{u}_a) = 0 \tag{3.2.2}$$

This is the equation of continuity, non-linear by nature. However, from the definition of condensation, the instantaneous mass density of air may be written as

$$\rho = \rho_o (1+s)\,, \tag{3.2.3}$$

where ρ_o is the constant ambient mass density and s is very small, which linearizes the non-linear equation of continuity as

$$\frac{\partial s}{\partial t} + \nabla \cdot \vec{u}_a = 0 \tag{3.2.4}$$

This equation can be integrated with respect to time to relate the condensation with fluid particle displacements, ξ_{ai}, as follows

$$s = -\nabla \cdot \vec{\xi}_a \tag{3.2.5}$$

since, $\int \nabla \cdot \vec{u}_a \, dt = \nabla \cdot \int \vec{u}_a \, dt = \nabla \cdot \int \left(\partial \vec{\xi}_a / \partial t\right) dt = \nabla \cdot \vec{\xi}_a$, and the constant of integration is zero, because the acoustic quantities are all zero if there is no disturbance present. The quantity $\vec{\xi}_a$ is the fluid particle displacement vector. Eliminating the condensation term from Eq. (3.2.1b) and Eq. (3.2.5), the following relation is obtained

$$p = -B \nabla \cdot \vec{\xi}_a \tag{3.2.6}$$

To derive the equation of dynamic equilibrium, the acoustic fluid is assumed to be inviscid and the effect of thermal conductivity is neglected. A fluid element $dV = dx\, dy\, dz$, which moves with the fluid, containing a mass of dm is considered. The net force $d\vec{f}$ on the element accelerates it according to the Newton's second law of motion. In the absence of viscosity, the net force on the element along x direction is

$$df_x = \left[P - \left(P + \frac{\partial P}{\partial x} dx \right) \right] dy\, dz = -\frac{\partial P}{\partial x} dV$$

Thus, the total force on the fluid element is

$$d\vec{f} = -\nabla P \, dV$$

The acceleration of the fluid element is

$$\vec{a} = \frac{\partial \vec{u}_a}{\partial t} + \frac{\partial \vec{u}_a}{\partial x} u_{ax} + \frac{\partial \vec{u}_a}{\partial y} u_{ay} + \frac{\partial \vec{u}_a}{\partial z} u_{az} = \frac{\partial \vec{u}_a}{\partial t} + \left(\vec{u}_a \cdot \nabla\right) \vec{u}_a \, .$$

The mass of the fluid element is $dm = \rho \, dV$. Hence the force equation becomes

$$-\nabla P = \rho \left[\frac{\partial \vec{u}_a}{\partial t} + \left(\vec{u}_a \cdot \nabla\right) \vec{u}_a \right]$$

This nonlinear, inviscid force equation is referred to as the Euler's equation. However, since s is negligible and $\left|(\vec{u}_a \cdot \nabla)\vec{u}_a\right| << \left|\partial \vec{u}_a / \partial t\right|$, due to their low numeric values, therefore ρ can be replaced by ρ_o and the term $(\vec{u}_a \cdot \nabla)\vec{u}_a$ can be dropped, and the linear, inviscid force equation results as follows

$$\rho_o \frac{\partial \vec{u}_a}{\partial t} = -\nabla p \tag{3.2.7}$$

The equations of state (3.2.1b), continuity (3.2.4), and force (3.2.7) can now be clubbed into a single differential equation with one dependent variable. The particle velocity can be eliminated between Eq. (3.2.4) and Eq. (3.2.7). Taking the divergence of Eq. (3.2.7)

$$\rho_0 \nabla \cdot \frac{\partial \vec{u}_a}{\partial t} = -\nabla^2 p$$

Similarly, taking the time derivative of Eq. (3.2.4),

$$\frac{\partial^2 s}{\partial t^2} + \nabla \cdot \frac{\partial \vec{u}_a}{\partial t} = 0$$

Eliminating $\vec{u}_a$ from these two relations produces

$$\nabla^2 p = \rho_o \left(\partial^2 s / \partial t^2\right).$$

Now the equation of state (3.2.1b) is used to eliminate the condensation term from the equation above, whereby

$$\nabla^2 p = \frac{1}{c^2} \frac{\partial^2 p}{\partial t^2}; \; c = \left(\sqrt{B / \rho_o}\right) \tag{3.2.8}$$

This is the three-dimensional lossless wave equation. The one-dimensional equivalent of this equation, travelling along the *z*- direction, may be written as

$$\frac{\partial^2 p}{\partial z^2} = \frac{1}{c^2}\frac{\partial^2 p}{\partial t^2} \tag{3.2.9}$$

where $p = p(z,t)$. In the above equations, variable c is the speed of propagation of sound through the acoustic fluid medium. Any function, with argument ($ct \pm z$), is a solution to Eq. (3.2.9). A solution, $f(ct-z)$ progresses towards the positive z direction, while the function $f(ct+z)$ advances in the negative z direction.

If it is now assumed that the medium is excited by a time-harmonic loading with a forcing frequency Ω such that

$$p(z,t) = p(z)\ \exp(i\Omega t),\ u_a(z,t) = u_a(z)\exp(i\Omega t) \tag{3.2.10}$$

then, Eq. (3.2.9) becomes

$$p_{,zz} - \frac{1}{c^2}\ddot{p} \equiv \left\{\frac{\partial^2 p(z)}{\partial z^2} + \frac{\Omega^2}{c^2}\ p(z)\right\}e^{i\Omega t} = 0 \tag{3.2.11}$$

Or, $\left(\dfrac{\partial^2 p}{\partial z^2}\right) + \dfrac{\Omega^2}{c^2}\ p = 0$ (3.2.12a)

Or, $\left(\dfrac{\partial^2 p}{\partial z^2}\right) + k^2 p = 0$ (3.2.12b)

Eq. (3.2.12) is the one-dimensional Helmholtz equation. The ratio $k = \Omega/c$, is referred to as wavenumber.

The velocity (Neumann) boundary condition for the one-dimensional Helmholtz equation can be derived from the kinetic condition obtained from Eq. (3.2.7). The one-dimensional kinetic relation will be

$$\rho_o \frac{\partial \vec{u}_a}{\partial t} = -\frac{\partial p}{\partial z}.$$

By inserting relations (3.2.10) in it, the following relation is obtained:

$$\frac{\partial p(z)}{\partial z} e^{i\Omega t} = -\rho_o \frac{\partial}{\partial t}\left(u_a(z) e^{i\Omega t}\right)$$

Or, $\frac{\partial p(z)}{\partial z} e^{i\Omega t} = -i\Omega\rho_o u_a(z) e^{i\Omega t}$

Finally, eliminating the time variable, time, at boundary it is seen that

$$\frac{\partial p(z)}{\partial z} = -i\Omega\rho_o u_a(z) \tag{3.2.13}$$

The three-dimensional Helmholtz equation is similarly derived and reads as follows

$$\left(\nabla^2 + k^2\right)p = 0 \tag{3.2.14}$$

where ∇^2 is the Laplacian operator, given by

$$\nabla^2 = \frac{\partial^2}{\partial x^2} + \frac{\partial^2}{\partial y^2} + \frac{\partial^2}{\partial z^2} \tag{3.2.15}$$

The Green's fundamental solution is deduced from the inhomogeneous Helmholtz equation in Section 3.4.

3.3 ASSUMPTIONS FOR THE ACOUSTIC PROCESS

The assumptions made in the theoretical acoustic formulation are listed below:

1. Only small-amplitude waves are taken under consideration in the present study. Hence the variation in density is small. The numerical values of condensation and the spatial derivatives of fluid particle displacements are also very close to zero.
2. The behaviour of the acoustic fluid has been assumed to be linear and inviscid.
3. Since the fluid is inviscid, the fluid motion is irrotational and the existence of a velocity potential for the fluid particles may be assumed for mathematical simplicity. However, here the analysis uses a pressure-velocity formulation for better physical understanding.
4. It is assumed that there is no flow in the acoustic medium.
5. The amplitude of the displacements and velocities at the boundary are also assumed to be of small amplitude.
6. The effect of gravity is neglected.

3.4 THE GREEN'S FUNCTION (FUNDAMENTAL SOLUTION)

The pressure response for a steady state harmonic acoustic problem in an infinite acoustic medium due to a unit point source is known as the so-called fundamental solution or Green's function, p^*. This is derived from the inhomogeneous Helmholtz equation where the inhomogeneous (source) term is a Dirac delta function that turns on only at the origin, *P*, of the reference frame that is being used. The equation reads:

$$\left(\nabla^2 + k^2\right)p^* + \delta(r) = 0 \tag{3.4.1}$$

Omitting the time dependence and following radial symmetry, $p^* = A_1 r^{-1} e^{-ikr}$, should be the nature of solution for the Green's function. Here, $i = \sqrt{-1}$, r is the distance between the acoustic source point, *P*, and the point of observation, *Q*, and A_1 is a constant, yet to be evaluated. This equation can be integrated over the entire infinite domain *V* as

$$\int_V \left(\nabla^2 + k^2\right)p^* dV = -\int_V \delta(r)\, dV = -1 \tag{3.4.2}$$

For a function of radial symmetry, the volume integration of Eq. (3.4.2), over a spherical volume of radius a, simplifies to (Fig. 3.4.1)

$$\int_V f(r)dV = \int_{r=0}^{a} \int_{\theta=0}^{2\pi} \int_{\phi=0}^{\pi} f(r) r^2 \sin\phi\, d\phi\; d\theta\, dr = 4\pi \int_0^a f(r)\, r^2 dr \tag{3.4.3}$$

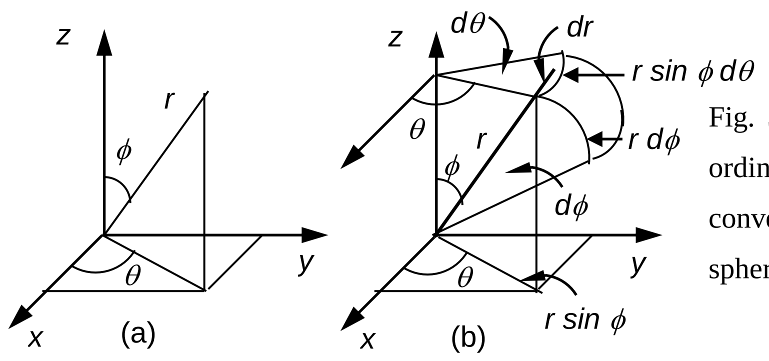

Fig. 3.4.1: (a) The spherical co-ordinate system, and (b) the conversion from Cartesian to spherical co-ordinates.

It may be noted that 4π is the solid angle subtended by the sphere at its centre. Substituting the left-hand-side of Eq. (3.4.2) into Eq. (3.4.3), for the function *f(r)*, it is found that

$$\int_V \left(\nabla^2 + k^2\right) p^* dV = A_1 \int_V \left\{\nabla^2\left(r^{-1}e^{-ikr}\right) + k^2\left(r^{-1}e^{-ikr}\right)\right\} dV = I + II \tag{3.4.4}$$

The second integral, *II*, is

$$II = 4\pi A_1 k^2 \int_0^a e^{-ikr} r\,dr = 4\pi A_1 \left\{ e^{-ika}(1+ika) - 1 \right\} \tag{3.4.5a}$$

To evaluate the first integral, *I*, the divergence theorem is applied as follows:

$$I = A_1 \int_V \vec{\nabla} \cdot \vec{\nabla}\left(r^{-1} e^{-ikr}\right) dV = A_1 \int_S \vec{\nabla}\left(r^{-1} e^{-ikr}\right) \cdot \hat{n}\, dS$$

$$= A_1 \int_S \frac{d}{dr}\left(r^{-1} e^{-ikr}\right) \hat{e}_r \cdot \hat{e}_r\, dS$$

$$= 4\pi A_1 e^{-ika}(-1 - ika) \tag{3.4.5b}$$

Combining Eqs. (3.4.5a) and (3.4.5b)

$$I + II = -4\pi A_1 = -1;\, A_1 = \frac{1}{4\pi},$$

or, $$p^* = \frac{e^{-ikr}}{4\pi r} \tag{3.4.6}$$

This is the desired Green's function, or the fundamental solution, for the harmonic acoustic problems. The directional derivatives of the fundamental solution for pressure are also needed to derive the fundamental solution for velocity. This is found as follows:

$$\frac{\partial p^*}{\partial x_j} = p^*_{,j} = -\frac{1}{4\pi r^2}\left[1 + ikr\right] r_{,j} e^{-ikr} \tag{3.4.7}$$

and,

$$\frac{\partial p^*}{\partial n} = p^*_{,n} = p^*_{,j} n_j = -\frac{1}{4\pi r^2}\left[1 + ikr\right] r_{,j} n_j e^{-ikr} \tag{3.4.8}$$

It may be noted that the functions in Eqs. (3.4.6)-(3.4.8) are singular, as *r* tends to zero, i.e, as the observation point tends to merge with the source point, the functions blow up infinitely. Now, that the Green's solution is known, the formulation for the Kirchhoff-Helmholtz integral equation can be attempted for an acoustic domain, as provided in the next section.

3.5 ACOUSTIC BOUNDARY INTEGRAL FORMULATION

The symmetric identity of Green, as given below, is considered to be the stepping stone to derive the boundary integral equation for the acoustic problems.

$$\int_V \left(\nabla^2 f\right) g\, dV - \int_V \left(\nabla^2 g\right) f\, dV = \int_S \left(g\,\nabla f - f\,\nabla g\right)\cdot \hat{n}\, dS \qquad (3.5.1)$$

It is required in this expression that the functions *f* and *g* and their first and second partial derivatives with respect to the spatial co-ordinates be continuous. The vector $\hat{n}$ is the unit outward normal to surface *S* containing a domain of interest, *V*. Now, it is assumed that the function *g* denotes the unknown acoustic pressure at any point in *V* or on *S*, and *f* is the Green's function. These functions satisfy the above identity at every point inside the domain and on the surface excepting the point of application of the acoustic source (since the Green's function becomes infinite at *r = 0*, but remains regular elsewhere). To deal with this singularity at the source, a small spherical domain, V_ε, of radius ε, centred at the source point P, and surrounded by surface S_ε, is excluded from the domain of interest *V* (refer Fig. 3.5.1). Gradually, this radius ε is forced to tend zero, to eliminate the singularity. In the process, Eq. (3.5.1) becomes

$$\int_{V-V_\varepsilon} \left(p\nabla^2 p^* - p^*\nabla^2 p\right) dV = \int_{S+S_\varepsilon} \left(p\frac{\partial p^*}{\partial n} - p^*\frac{\partial p}{\partial n}\right) dS$$

Since within the domain *V-V*$_\varepsilon$, $\nabla^2 p = -k^2 p$ and $\nabla^2 p^* = -k^2 p^*$, the left-hand-side of the above equation is identically zero. Thus, the above equation becomes

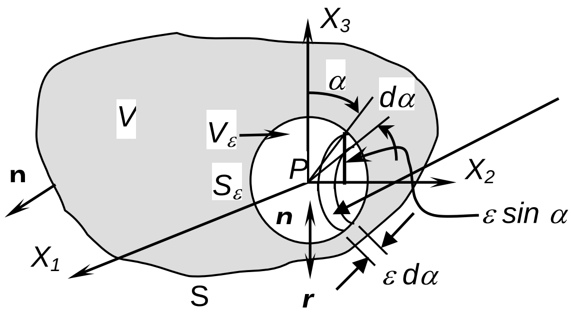

Area of the ring element
= $2\pi\,(\varepsilon\, sin\ \alpha)\,(\varepsilon\, d\alpha)$.

Figure 3.5.1. Integration around source point in polar coordinates.

$$\int_{S_\varepsilon}\left(p\frac{\partial p^*}{\partial n} - p^*\frac{\partial p}{\partial n}\right) dS + \int_{S}\left(p\frac{\partial p^*}{\partial n} - p^*\frac{\partial p}{\partial n}\right) dS = I + II = 0 \qquad (3.5.2)$$

On S_ε, $\partial/\partial n = -\partial/\partial r$. Hence,

$$\begin{aligned} I &= \int_0^\pi \left(p\frac{\partial p^*}{\partial n} - p^*\frac{\partial p}{\partial n}\right) 2\pi\, r^2 \sin\alpha\, d\alpha \\ &= \int_0^\pi -\left(p\frac{\partial p^*}{\partial r} - p^*\frac{\partial p}{\partial r}\right) 2\pi\, r^2 \sin\alpha\, d\alpha \end{aligned}$$

Now $p^* = e^{-ikr}/4\pi r$; $p^*_{,r} = \dfrac{1}{4\pi}\left(-r^{-2}e^{-ikr} - r^{-1}e^{-ikr}\cdot ik\right)$. Hence,

$$I = Lt_{\ \varepsilon\to 0}\frac{-1}{4\pi}\int_0^\pi \left\{ p(P)\left(\frac{.e^{-ik\varepsilon}\left(1+ikr\right)}{\varepsilon^2}\right) + \frac{e^{-ik\varepsilon}}{\varepsilon}\frac{\partial p(P)}{\partial n}\right\} 2\pi\varepsilon^2 \sin\alpha\, d\alpha$$

$$= -p(P)$$

Substituting this result back into Eq. (3.5.2) it is found that

$$\begin{aligned} &-p(P) + \int_S \left(p\frac{\partial p^*}{\partial n}\right) dS - \int_S \left(p^*\frac{\partial p}{\partial n}\right) dS = 0 \\ &\therefore\ p(P) - \int_S \left(p\frac{\partial p^*}{\partial n}\right) dS = -\int_S \left(p^*\frac{\partial p}{\partial n}\right) dS \end{aligned} \qquad (3.5.3)$$

Thus the integral equation (3.5.3), valid for any point inside the acoustic domain has been achieved. In the boundary element method it is preferred for computational reasons to take the observation points to the boundary *S*. This is done simply by taking the source point *P* to the boundary and augment the domain by a hemisphere of radius ε (in three-dimensions at *P*) as shown in Fig. 3.5.2. The point *P* is in the centre of the hemisphere, and, in the limit, the radius of the hemisphere is forced to approach zero.

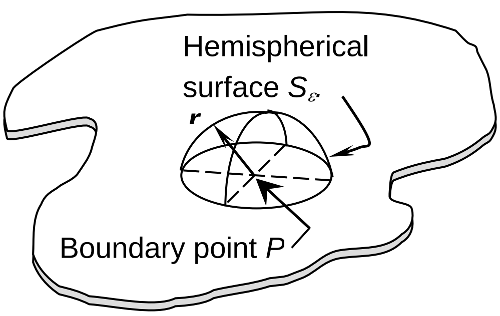

Figure 3.5.2. Taking the integral equation to the boundary.

Thus P becomes a point on the boundary and the resulting equation becomes a boundary integral equation (BIE). Presently, only a smooth boundary at P is considered. The cases of edges and corners are discussed at a later stage.

It is important at this stage to differentiate between the two types of kernel that are present in Eq. (3.5.3) since the kernel containing the fundamental solution, p^* and that containing its derivative behave differently. The integrals are easy to deal with, as the order of singularity is $O(1/r)$ [34]. For example:

$$Lt_{\varepsilon\to 0}\left\{\int_{S_\varepsilon} p^* \frac{\partial p}{\partial n} dS\right\} = Lt_{\varepsilon\to 0}\left\{-\int_{S_\varepsilon} \frac{e^{-ikr}}{4\pi r}\frac{\partial p}{\partial r} dS\right\} = Lt_{\varepsilon\to 0}\left\{-\int_{S_\varepsilon} \frac{e^{-ik\varepsilon}}{4\pi\varepsilon}\frac{\partial p(P)}{\partial r} dS\right\}$$

$$= Lt_{\varepsilon\to 0}\left\{-\frac{e^{-ik\varepsilon}}{4\pi\varepsilon}\left.\frac{\partial p(P)}{\partial r}\right|_{r=\varepsilon}\left(\psi\varepsilon^2\right)\right\} = Lt_{\varepsilon\to 0} f\{O(\varepsilon)\} = 0$$

In other words, the right-hand side integral in Eq. (3.5.3) is continuous when both the source and the field points are taken to the boundary. It may be noted that ψ is the solid angle that is subtended by the surface S at P. The left-hand side integral, however, behaves in a separate manner. Here, around S_ε one has the following results:

$$Lt_{\varepsilon\to 0}\int_{S_\varepsilon} p\frac{\partial p^*}{\partial n} dS = Lt_{\varepsilon\to 0}\int_{S_\varepsilon} p(P)\frac{e^{-ik\varepsilon}}{4\pi\varepsilon^2}(1+ik\varepsilon)dS = Lt_{\varepsilon\to 0}\, p(P)\frac{e^{-ik\varepsilon}}{4\pi\varepsilon^2}(1+ik\varepsilon)\psi\varepsilon^2$$

$$= \frac{\psi}{4\pi}\, p(P) = C(P)\, p(P) \tag{3.5.4}$$

Thus Eq. (3.5.3) can be rewritten as a truly boundary integral equation

$$C(P)\,p(P) + \int_S\left(p\frac{\partial p^*}{\partial n}\right)dS = \int_S\left(p^*\frac{\partial p}{\partial n}\right)dS \tag{3.5.5}$$

Equation (3.5.5) can be modified to replace the pressure derivative by the normal particle velocity, which is a more useful quantity. For the time harmonic cases, the momentum-balance equation that relates the normal fluid particle velocity, u_{an}, velocity and the normal pressure derivative on the boundary can be written in light of Eq. (3.2.13) as follows:

$$u_{an} = -\frac{1}{i\rho_o\Omega}\frac{\partial p}{\partial n} \tag{3.5.6}$$

where, ρ_o is the density of the acoustic medium. Hence, Eq. (3.5.5) is rewritten as

$$C(P)\,p(P) + \int_S p(Q)\left(\frac{\partial p^*(P,Q)}{\partial n_Q}\right) dS_Q = \int_S u_{an}(Q)\left(-i\Omega\,\rho_o\,p^*\right)dS_Q \tag{3.5.7}$$

The constant *C(P)* can be evaluated from the potential problem for the same fluid domain, when subjected to an equipotential condition throughout the domain, as follows:

For a potential problem for the same domain, with governing equation $\nabla^2 U = 0$ and Green's function $U^* = 1/4\pi\, r$, with reference to Figs. (3.5.1) and (3.5.2), the integral equation form equivalent to acoustic integral equation (3.5.2) may be written as

$$\int_S \left(\frac{1}{4\pi r}\frac{\partial U}{\partial n} - U\frac{\partial}{\partial n}\left(\frac{1}{4\pi r}\right)\right)dS = \int_{S_\varepsilon}\left(\frac{1}{4\pi r}\frac{\partial U}{\partial r} - U\frac{\partial}{\partial r}\left(\frac{1}{4\pi r}\right)\right)dS$$

The first term in the right-hand side is again zero since the integrand is $O(\varepsilon)$, and $\varepsilon \to 0$. Thus this equation reduces to:

$$\int_{S_\varepsilon} -U\frac{\partial}{\partial r}\left(\frac{1}{4\pi r}\right) = C(P)U(P) = \int_S \left(\frac{1}{4\pi r}\frac{\partial U}{\partial n} - U\frac{\partial}{\partial n}\left(\frac{1}{4\pi r}\right)\right)dS \tag{3.5.8}$$

The required value for $C(P)$ can be obtained from Eq. (3.5.8) and used in Eq. (3.5.7), by imposing a special case where potential $U = 1$ throughout the domain V. This gives:

$$\int_{S_\varepsilon} -1\frac{\partial}{\partial r}\left(\frac{1}{4\pi r}\right) = C(P)\cdot 1 = \int_S \left(\frac{1}{4\pi r}\cdot 0 - 1\frac{\partial}{\partial n}\left(\frac{1}{4\pi r}\right)\right)dS$$

$$C(P) = \int_S -\frac{\partial}{\partial n}\left(\frac{1}{4\pi r}\right)dS \tag{3.5.9}$$

This value for *C(P)* can be used in Eq. (3.5.7), so that the equation becomes practically applicable for all acoustic cavities for interior problem. For exterior acoustic analysis

$$C'(P) = 1 - \int_S -\frac{\partial}{\partial n}\left(\frac{1}{4\pi r}\right)dS \tag{3.5.10}$$

3.6 ISOPARAMETRIC BOUNDARY ELEMENT FORMULATION

To solve the problems numerically, the boundary surface is divided into discrete elements and some nodal points define each element. In this case, it is assumed that the surface is discretized into *ne* number of eight-noded surface elements, and there are *nn* nodes in all. Isoparametric serendipity shape functions, identical to those provided in Fig. 2.11.1(b) are used to interpolate the intra-element co-ordinates and acoustic variables from the nodal values of the corresponding elements as shown below:

$$\begin{aligned} x_i &= \sum_{j=1}^{8} N_j(\xi_1,\xi_2)(x_i)_j \,;\; i = 1,2,3 \\ p &= \sum_{j=1}^{8} N_j(\xi_1,\xi_2)(p)_j \\ u_{an} &= \sum_{j=1}^{8} N_j(\xi_1,\xi_2)(u_{an})_j \end{aligned} \qquad (3.6.1)$$

Here x_i are the Cartesian co-ordinate terms, p is the acoustic pressure and u_{an} is the fluid particle velocity at the surface along the normal to the surface. Here ξ_1 and ξ_2 are the intrinsic co-ordinates (refer Fig. 3.7.1), each having a limit of ±1. This transformation is needed to implement Gauss quadrature for the numerical evaluation of the integration of the kernel functions. The discretized form of equation (3.5.7) is given below

$$\begin{aligned} & C(P)p(P) + \sum_{m=1}^{ne}\sum_{l=1}^{8}\int_{-1}^{+1}\int_{-1}^{+1}\frac{\partial p^*}{\partial n}(P,Q)N_l(\xi_1,\xi_2)\,p_l(Q)\left|J(\xi_1,\xi_2)\right|d\xi_1 d\xi_2 \\ & = \sum_{m=1}^{ne}\sum_{l=1}^{8}\int_{-1}^{+1}\int_{-1}^{+1}[-i\Omega\rho p^*(P,Q)]N_l(\xi_1,\xi_2)\,u_{anl}(Q)\left|J(\xi_1,\xi_2)\right|d\xi_1 d\xi_2 \end{aligned} \qquad (3.6.3)$$

Here $|J|$ is the determinant of the Jacobian matrix of transformation from x_i Cartesian co-ordinates to (ξ_1, ξ_2) local co-ordinates, and N_l are the shape functions for an eight-noded surface element. The normal direction $\vec{n}$ to the boundary at point Q is obtained by the cross product of the surface tangent vectors at the point Q,

$$\vec{n} = \frac{\partial \vec{r}}{\partial \xi_1} \times \frac{\partial \vec{r}}{\partial \xi_2}\,;\; \vec{r} = x_1\hat{i} + x_2\hat{j} + x_3\hat{k}\,;\;\; x_i = (x_i)_j N_j\,,\; j = 1,2,..,8 \qquad (3.6.4)$$

Since the area vector of an infinitesimal area on an element is given as

$$d\vec{A} = \vec{r}_{,\xi_1} \times \vec{r}_{,\xi_2} = \begin{vmatrix} \hat{i} & \hat{j} & \hat{k} \\ \dfrac{\partial x}{\partial \xi_1} & \dfrac{\partial y}{\partial \xi_1} & \dfrac{\partial z}{\partial \xi_1} \\ \dfrac{\partial x}{\partial \xi_2} & \dfrac{\partial y}{\partial \xi_2} & \dfrac{\partial z}{\partial \xi_2} \end{vmatrix} d\xi_1 d\xi_2 = \left(n_x\hat{i} + n_y\hat{j} + n_z\hat{k}\right) d\xi_1 d\xi_2 = (dA)\hat{n}\,. \qquad (3.6.5)$$

so, the Jacobian of transformation, $|J|$, is given by the magnitude of the normal vector $\vec{n}$

$$\left|J(\xi_1,\xi_2)\right| = \sqrt{n_x^2 + n_y^2 + n_z^2}\,, \qquad (3.6.6)$$

In equation (3.6.3) the Gauss-Legendre quadrature is applied to integrate the kernel. Each node of the BE mesh is made to assume the role of point P and a boundary element equation is found from Eq. (3.6.3). The number of equations thus derived is *nn*. Upon assembly a set of linear algebraic equation results and may be expressed as

$$[H]\{p\} = [G]\{u_{an}\} \tag{3.6.7}$$

This is the system equation for an acoustic enclosure. At a node connected to r number of elements, there are essentially r velocity terms whose magnitude and direction may be independent. The pressure terms are however scalar quantities. Hence, $[H]_{\mathrm{nn\ x\ nn}}$ is a square matrix due to full assembly, while $[G]_{\mathrm{nn\ x\ 8ne}}$ remains a rectangular one, being not fully assembled. These complications and the difficulty of evaluating the value of coefficient *C(P)*, however, may be avoided by the use of constant elements .

3.7 REGULAR AND SINGULAR KERNEL INTEGRALS

When the field point Q and the source point P lie on separate elements, the distance between these points, $r(P,Q)$, is nonzero and finite. Hence the Green's functions are regular or non-singular. Thus the integrand in Eq. (3.6.3) can be evaluated without difficulty.

However, when P and Q lie on same element, for certain Gauss points, the quantity $r(P,Q)$ tends to be zero and the Green's functions, p^* and $\partial p^* / \partial n$ tend to become singular since they are of the order *1/r* (The quantity p^* has a denominator involving distance $r(P,Q)$, while its normal derivative has $\{r(P,Q)\}^2$. However, the latter term involves a coefficient $\partial r / \partial n$ which is of the order $r(P,Q)$ [34]. Hence a transformation equivalent to a polar transformation is used, where the elemental area term, *dS*, in the numerator is replaced by a "$r\,dr\,d\theta$" -type term, which nullifies the *1/r* singularity. This is done by subdividing the elements, as shown in Fig. 3.7.1, into triangular sub-elements (Fig. 3.7.2) with point P at the vertices of all sub-elements. The triangular sub-elements are imagined as four noded linear elements, by clubbing nodes 1 and 2 of the linear quadrilateral element together at point P.

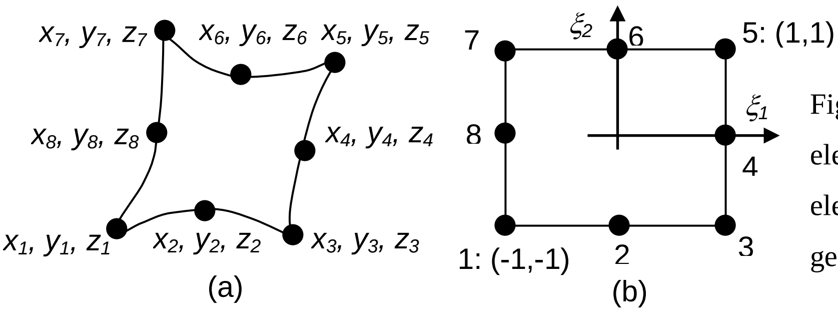

Figure 3.7.1 Serendipity element. (a) The parent element, and (b) the generic element.

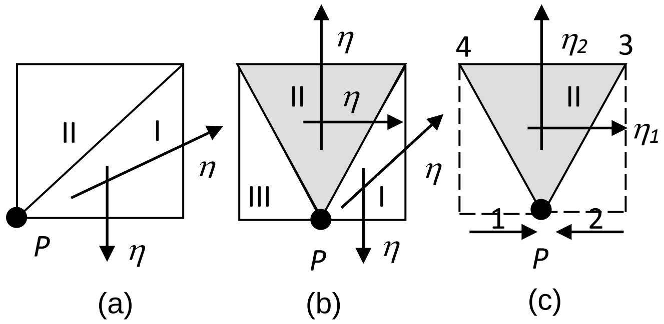

Figure 3.7.2 Singular integration over elements, done by subdividing them into sub-elements.

The first two nodes are assumed to be concentrated at the singular point P, whereas the other two nodes are at the remaining vertices of the concerned sub-element, as shown in Fig. 3.7.2. The linear shape functions used are as shown below:

$$
\begin{aligned}
L_1(\eta_1,\eta_2) &= (1-\eta_1)(1-\eta_2)/4 \\
L_2(\eta_1,\eta_2) &= (1+\eta_1)(1-\eta_2)/4 \\
L_3(\eta_1,\eta_2) &= (1+\eta_1)(1+\eta_2)/4 \\
L_4(\eta_1,\eta_2) &= (1-\eta_1)(1+\eta_2)/4
\end{aligned}
\tag{3.7.1}
$$

This is a non-linear transformation. By this transformation the lines η = +1 and η = -1 converge at point P making the Jacobian $J(\eta_1 , \eta_2)$ of the order r [34]. In the vicinity of P, the shape function is of the order r , while the Green's functions p^* and $\partial p^*/\partial n$ are of the orders $1/r$. Hence the products of kernel, shape function and Jacobian tend to a finite limit as points P and Q approaches each other, and the integrands can be evaluated using the standard Gauss quadrature. By the application of this transformation the integrands are integrated as follows:

$$
\begin{aligned}
\int_S f(P,Q)dS &= \int_{-1}^{1}\int_{-1}^{1} f(\xi_1,\xi_2)\left|J(\xi_1,\xi_2)\right| \, d\xi_1 d\xi_2 \\
&= \int_{-1}^{1}\int_{-1}^{1} f(\eta_1,\eta_2)\left|J(\xi_1,\xi_2)\right| \, \left|J(\eta_1,\eta_2)\right| \, d\eta_1 d\eta_2
\end{aligned}
\tag{3.7.2}
$$

3.8 INTERIOR ACOUSTIC ANALYSIS OF RIGID CAVITY

For rigid cavity problem, the normal particle velocity at the boundary is zero. Absorbent layers may be added to the boundaries to reduce noise inside the acoustic cavity, V. To accommodate the velocity boundary condition, a reorientation of the system Eq. (3.6.3) has to be made before applying Gauss elimination.

On boundary, let the measured amplitude of the fluid particle velocity normal to the boundary is specified along with the forcing frequency Ω. Let u_s be the normal velocity of the structural boundary as illustrated in Figure 3.8.1. Due to the presence of the absorbent material, the magnitude of the fluid particle velocity, u_a, at the boundary is different from the structural velocity. The relative fluid particle velocity, u_r, referenced to structural surface is given by

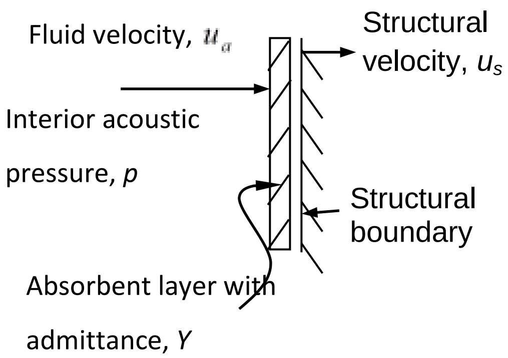

Figure 3.8.1. Moving boundary with normal velocity u_s, with surface acoustic admittance Y specified.

$$u_r = u_a - u_s, \tag{3.8.1}$$

The relation between the relative velocity, u_r, and the acoustic pressure, p, can be represented through the experimentally obtained acoustic admittance term, Y, as [29]

$$u_r = Yp. \tag{3.8.2}$$

Hence, $u_a = Yp + u_s$ (3.8.3)

The acoustic admittance is measured in an impedance tube [29]. The admittance is the inverse of the acoustic impedance, the latter being defined as the ratio between pressure and normal fluid velocity at a point over a surface. The value of the acoustic admittance is taken to be zero on surfaces without absorbent layer.

In the present study only 30 mm thick polyurethane foam sheets will be applied as absorbent layers, and the values of the acoustic admittance has been obtained from Suzuki et a.l [29] and shown in Fig. 3.8.2.

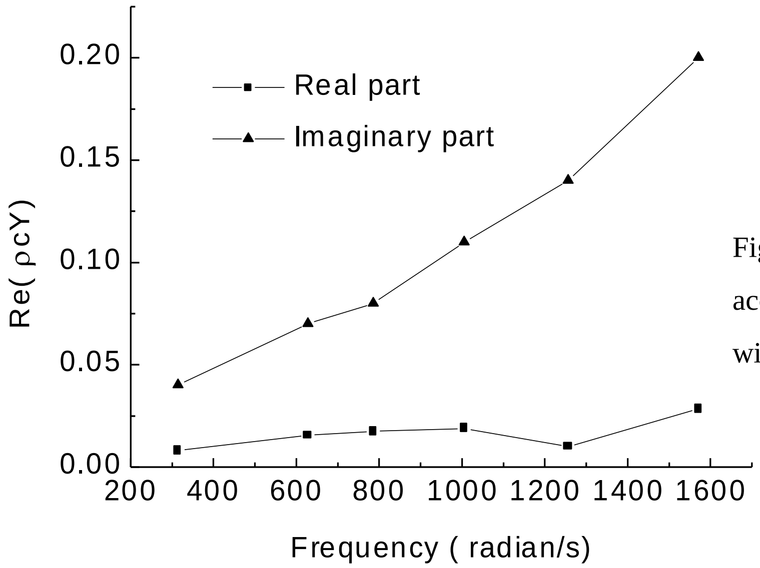

Figure 3.8.2 Non-dimensionalized acoustic admittance (ρcY) measured with impedance tube (Suzuki [29]).

Since the value of the admittance is frequency-dependent, a subroutine has been developed to interpolate the intermediate values for different forcing frequencies.

In this case no special effort is required to incorporate the velocity boundary condition. The system equation for BEM is given by

$$[H]\{p\} = [G]\{u_{an}\} \tag{3.8.4}$$

The coefficient matrix [H] is square while [G] is rectangular for reasons stated in Section 3.6. It may be recalled that the exact number of unknowns is equal to the number of equations available, i.e., equal to the order of matrix [H], or the number of nodes on the boundary, *nn*. Thus, the imminent objective is to get the unknown quantities to the left-hand side, inside vector {p}, and send the known quantities inside vector {u_{an}}. Upon matrix multiplication of the known quantities on the right hand side, the right-hand side becomes a known vector, and the equation can be solved via complex Gauss elimination. Since the velocity terms are already in the right-hand side, they need not be transported. However, it may be noted that the velocity terms in this equation are actually fluid particle velocity terms and not the structural velocity terms. Thus they are remodelled before incorporating the boundary values if the structural surface is provided with absorbent layers.

A specific equation may be taken to explain the methodology to incorporate the absorbent layer into the present computations. The j^{th} boundary element equation may be written as follows:

$$H_{j1}p_1+H_{j2}p_2+H_{j3}p_3+\ldots+H_{j(nn)}\,p_{nn}= G_{j\,1\text{-}1}u^a_{1\text{-}1}+G_{j\,1\text{-}2}\,u^a_{1\text{-}2}+\ldots+G_{j\,1\text{-}8}\,u^a_{1\text{-}8}\,+$$

$$G_{j\,2\text{-}1}u^a_{2\text{-}1}+G_{j\,2\text{-}2}\,u^a_{2\text{-}2}+\ldots+G_{j\,2\text{-}8}\,u^a_{2\text{-}8}+\ldots+ \qquad (3.8.5)$$

$$G_{j\,ne\text{-}1}u^a_{ne\text{-}1}+G_{j\,ne\text{-}2}\,u^a_{ne\text{-}2}+\ldots+G_{j\,ne\text{-}8}\,u^a_{ne\text{-}8}$$

In the above equation, it has been assumed that there are *nn* nodes and *ne* elements. Thus the system involves *nn* nodal pressure terms and *8*ne* nodal velocity terms in *nn* equations. H_{jk} means the coefficient of pressure, p_k, at global node number k in the j^{th} equation. Likewise, $G_{j\,k\text{-}l}$ means the coefficient of normal fluid particle velocity, $u^a_{k\text{-}l}$, on the $l^{\,th}$ local node of k^{th} global element, in equation number j.

Now the incorporation of absorbent layer property at one typical node may be discussed. The other cases are only prototypical. Let the first element be mounted with some absorbent layer with admittance Y, and let the discussion be confined only to its first local node. Then, assuming that the global node number of the first local node of the first element to be 1, Eq. (3.8.5) may be rewritten as

$$[H_{j1}-G_{j\,1\text{-}1}.Y].p_1+H_{j2}p_2+H_{j3}p_3+\ldots+H_{j(nn)}\,p_{nn}= G_{j\,1\text{-}1}(u^s_{1\text{-}1})+G_{j\,1\text{-}2}\,u^a_{1\text{-}2}+\ldots+G_{j\,1\text{-}8}\,u^a_{1\text{-}8}\,+$$

$$G_{j\,2\text{-}1}u^a_{2\text{-}1}+G_{j\,2\text{-}2}\,u^a_{2\text{-}2}+\ldots+G_{j\,2\text{-}8}\,u^a_{2\text{-}8}+$$

$$\ldots+G_{j\,ne\text{-}1}u^a_{ne\text{-}1}+G_{j\,ne\text{-}2}\,u^a_{ne\text{-}2}+\ldots+G_{j\,ne\text{-}8}\,u^a_{ne\text{-}8} \qquad (3.8.6)$$

A similar process may be applied for all local nodes of all elements with absorbent layers, to account for the difference between the fluid and structural velocities at the boundary with absorbent layers. Now, since the structural velocities are measurable, the velocity boundary conditions can be easily introduced.

3.9 EXTERIOR ACOUSTIC ANALYSIS

Boundary element methods have been used in acoustic radiation and scattering for decades [11-16, 18–20, 22]. The major advantage of boundary element methods over other numerical techniques is that only the surface of the body needs to be modelled. The Sommerfield radiation condition at infinity is automatically satisfied. However, one potential shortcoming is that the exterior boundary integral formulation, either direct or indirect, fails to produce a correct solution at a set of irregular frequencies associated with the eigen frequencies of the corresponding interior domain. For the direct BEM formulation, the problem is referred to as "the non-uniqueness difficulty," while for the indirect BEM formulation, the problem is often referred to as "the non-existence difficulty."

The non-uniqueness difficulty associated with the direct BEM is harder to explain from the physical ground because the integral equation used is for the exterior problem only, instead of a combined interior/exterior problem. Although the exterior domain and corresponding (imaginary) interior domain share the same boundary, the direct boundary integral equations for the exterior and the interior problems are still slightly different in two aspects (Fig. 3.9.1)

I. Their normal directions are opposite to each other, and
II. Their solid angles are different at corners and edges.

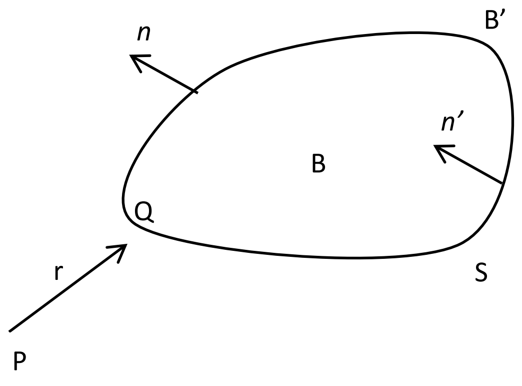

Figure 3.9.1 Graphical representation of acoustic problem, *B* is the domain and *n* is outward normal to the surface for interior acoustics, whereas *B'* is the domain and *n'* is outward normal to the surface for exterior acoustics, P and Q are source point and observation point respectively

It is hard to just directly compare the interior and exterior boundary integral equations to explain why the non-uniqueness difficulty would occur. Advanced mathematical explanations have been presented in papers more than half a century ago, cf. Kupradze [36] and Weyl [37].

A simple mathematical explanation of this phenomenon can be found in Wu and Seybert [38, 39] and later in Wu [40] as well. It has been shown that regardless of the type of boundary conditions prescribed for the exterior problem (Neumann, Dirichlet, or impedance), the Kirchhoff-Helmholtz integral equation will always fail to yield a unique solution at the eigen frequencies of the corresponding interior Dirichlet problem. In real world applications, knowing the exact locations of the irregular frequencies is actually not that important because it is impractical to solve an interior Dirichlet problem first just to find the eigen frequencies. A more reasonable approach is to always apply some kind of treatment in the direct BEM at every frequency to prevent the non-uniqueness from happening. Actually, at high frequencies, the eigen frequencies are so closely spaced that it is impossible to distinguish the regular frequencies from the irregular frequencies.

Over the last four or five decades, many different approaches were proposed to create a unique solution. Among them the two most popular categories are

I. the Combined Helmholtz Integral Equation Formulation (CHIEF) method originally proposed by Schenck [41] and its variations, and
II. The linear combination of the Kirchhoff-Helmholtz integral equation and its normal derivative originally proposed by Panic [42] and Brakhage and werner [43]. This approach was adopted to the Neumann problem by Burton and Miller [44].

From the above two methods the CHIEF method has been used in the case studies of the thesis.

3.10 CHIEF METHOD PROPOSED BY SCHENCK

The system of equations valid for BEM as derived previously can be written as (3.8.4)

$$[H]\{p\}=[G]\{u_{an}\}$$

We need to choose m collocation points located in the enclosed cavity. These points usually referred to as CHIEF points. The system matrix H corresponding to the CHIEF method takes the form [45]

$$
H = \left|\begin{array}{ccc}
c_1+\bar{h}_{11} & \bar{h}_{12} \;\dots & \bar{h}_{1n} \\
\bar{h}_{21} & c_2+\bar{h}_{22} \;\dots & \bar{h}_{2n} \\
\vdots & \vdots & \vdots \\
\bar{h}_{n1} & \bar{h}_{n2} \;\dots & c_n+\bar{h}_{nn} \\
\hline
\bar{h}_{n+11} & \bar{h}_{n+12} & \bar{h}_{n+1n} \\
\vdots & \vdots & \vdots \\
\bar{h}_{n+m1} & \bar{h}_{n+m2} & \bar{h}_{n+mn}
\end{array}\right|
$$

The rectangular system reflects the fact that we now have an over-determined linear system of algebraic equations for the n-dimensional vector of unknowns, p. this system is solved in a least square sense, where the unknown solution is formally given by

$$p = (H^H H)^{-1} H^H G \; u_{an}$$

with superscript ^{H} denoting hermitian, i.e. transposed conjugate complex matrix. There are a large number of publications on the use and variations of this popular method [18].

4. NUMERICAL RESULT

A MATLAB programme has been developed using boundary element method to solve exterior and interior acoustic problem. Eight noded isoparametric element is used in the analysis. The numerical analysis is divided in two parts. First part contains exterior acoustic analysis using CHIEF and second part contains interior acoustic analysis using absorbent layer.

4.1 EXTERIOR ACOUSTICS

Three case studies are shown in this part as follows.

- **a)** Case study of a pulsating sphere
- **b)** Case study of a pulsating cube
- **c)** Case study of a pulsating cylinder

4.1.1 CASE STUDY OF A PULSATING SPHERE

The simplest source to deal with mathematically with a finite volume velocity is called a monopole, a point source or a simple source. The acoustic source simplest to analyse is a pulsating sphere-a sphere whose radius varies sinusoidally with time. While pulsating spheres are of little practical importance, their analysis is useful for they serve as the prototype for an important class of sources referred to as simple sources.

The exact analytical solution for the acoustic pressure at a distance r from the center of a sphere (Fig. 4.1.1a) of radius a, pulsating with uniform radial velocity U_a is [46]

$$p(r) = (a/r)U_a[iz_o ka/(1+ika)]e^{[-ik(r-a)]} \quad (4.1.1a)$$

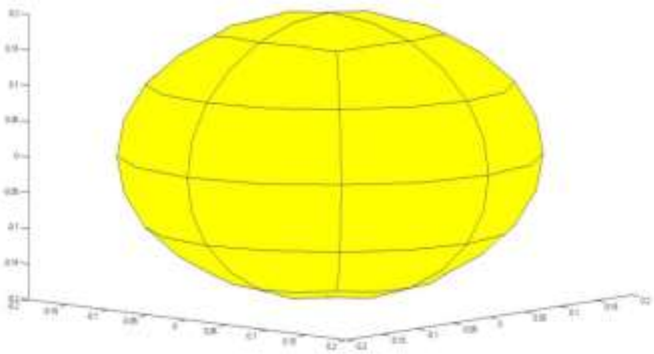

Fig.4.1.1a Pulsating Sphere

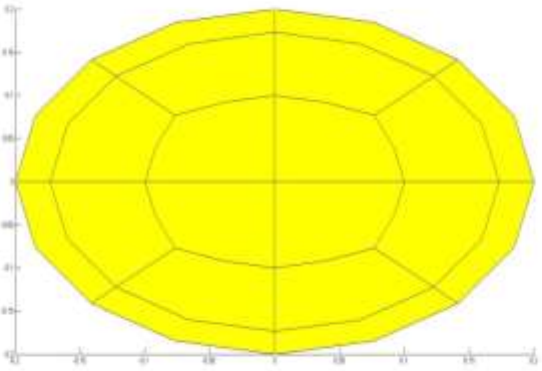

Fig.4.1.1b Showing Top Surface of Pulsating Sphere

The radius of the pulsating sphere is taken as 0.2m. It is divided into a total of 40 numbers of elements and of 122 total numbers of nodes. The normal velocity is taken as 0.001m/s throughout the surface.

A MATLAB programme is developed to find out the surface pressure of the Pulsating Sphere and with the help of CHIEF method the non-uniqueness problem relating to certain wavenumber has been tried to eliminate.

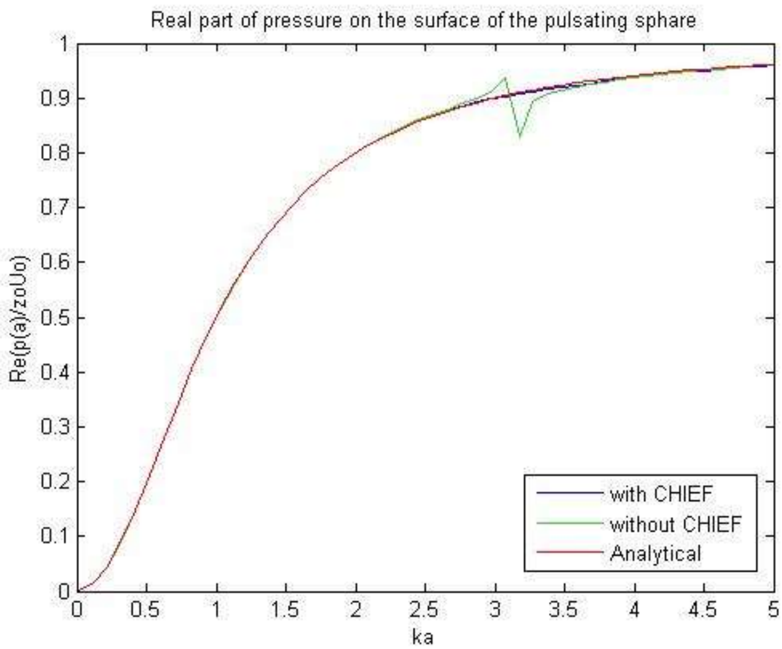

Fig.4.1.1c Real part of the pressure on the surface of a pulsating sphere

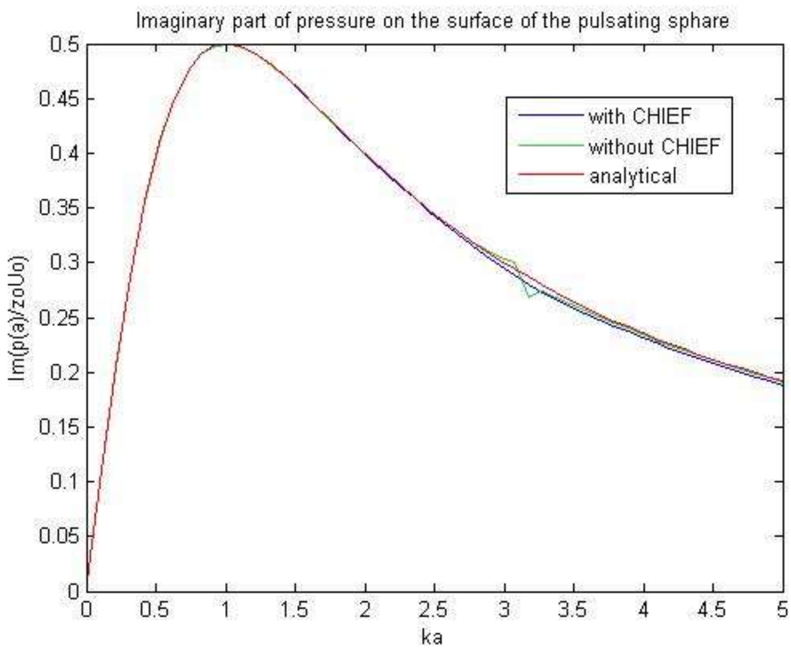

Fig.4.1.1d Imaginary part of the pressure on the surface of a pulsating sphere

Figure 4.1.1c and 4.1.1d are the plots of the real and imaginary parts of dimensionless acoustic pressure on the surface ($r = a$) of the pulsating sphere as a function of *ka*. The data in the neighbourhood of $ka = \pi$ (the first interior eigen frequency) have been improved by using a single CHIEF point located at the centre of the sphere. The plot shows well in agreement with the analytical results. Without CHIEF the results near the first interior eigen frequency contain a large error resulting from severe ill conditioning of over-determined system of equations available for solving in BEM.

4.1.2 CASE STUDY OF A CUBE

To show how well the boundary element method handles bodies with edges and corners a problem with cubical geometry is considered. The problem of a pulsating cube is formulated by prescribing the normal velocity on a cubical surface produced by a pulsating sphere of radius a circumscribed by the cube. The boundary condition on the cube is given by

$$((\partial\emptyset)/\partial n)_{cube} = -\nabla_n \frac{p(r)}{iz_o k} \tag{4.1.2a}$$

Here *p(r)* is given by Eq. 4.1.1a and *n* is the outward normal to the surface of the cube. The side of cube is taken as 0.4m, since it is formed circumscribing the sphere as in the previous case. Each side of the cube is divided into 4 x 4 numbers of elements and a total of 290 numbers of nodes. The CHIEF point is taken at the centre of the cube.

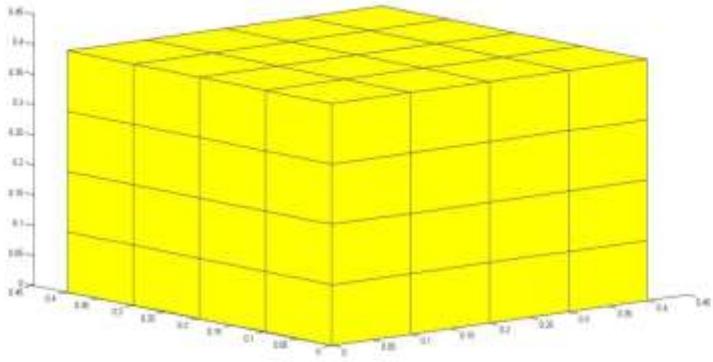

Fig.4.1.2a Geometry of Pulsating Cube

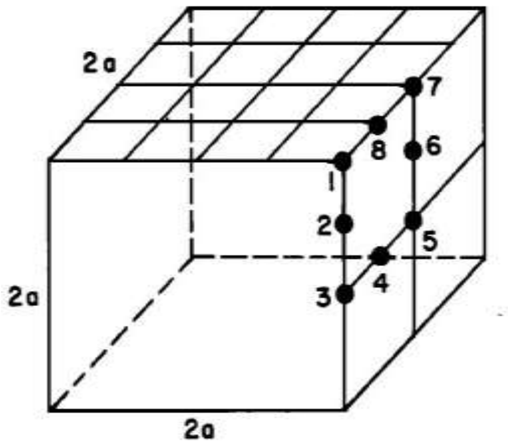

Fig.4.1.2b Nodes on the pulsating cube

The Normalized pressures on the nodes shown in the above figure are obtained using BEM with CHIEF with the help of MATLAB programming. The results obtained were shown in Table 4.1.2.The numerical values are compared with the theoretical value and it is seen that it very well matches with the analytical value.

Table 4.1.2. Normalized pressure magnitude $|p|/z_o U_a$ on the surface of a radiating cube for ka = 1

NODES	THEORETICAL VALUE	NUMERICAL RESULT FROM MATLAB
1	0.40824	0.408747
3,7	0.50000	0.497745
2,8	0.47140	0.470938
5	0.70711	0.688966
4.6	0.63246	0.622434

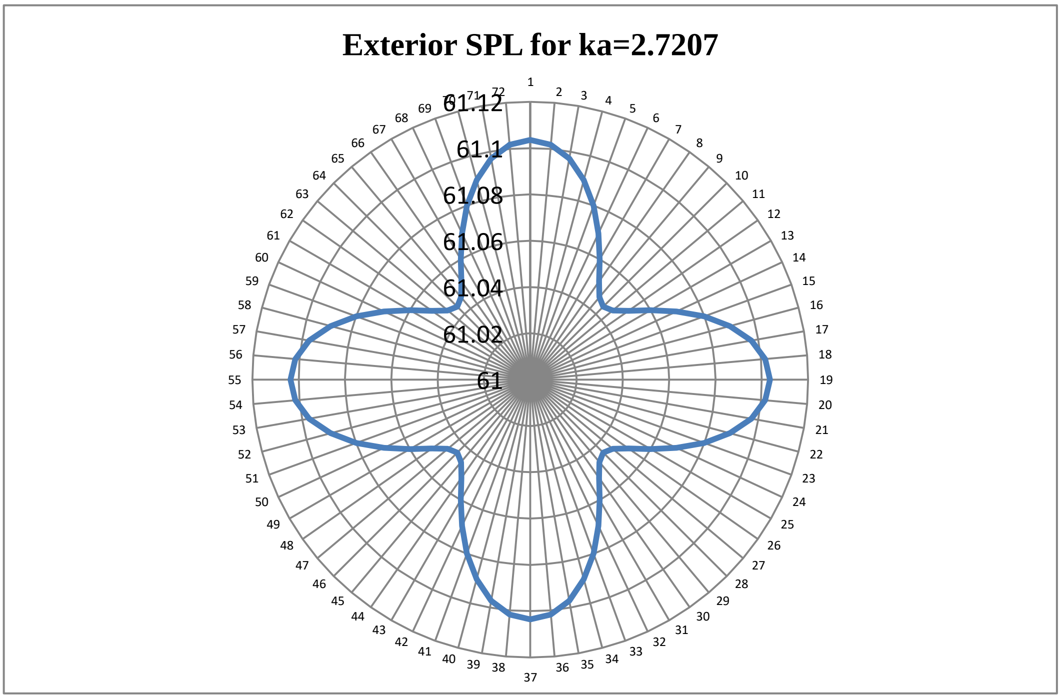

Fig.4.1.2c Farfield pressure magnitude patterns for a pulsating cube

The above figure shows the pattern of farfield pressure value for ka = 2.7207 (= $\sqrt{3}\pi/2$) [15] which is characteristic frequency for this cube taken at polar angle from the centre of the cube at distance of 2m (10a = 10*0.2).

4.1.3 CASE STUDY OF A CYLINDER

In this case we have done radiation from a finite circular cylinder. A uniform radial velocity of 0.001m/s is prescribed on the periphery of the cylinder. The ends of the cylinder are considered motionless.

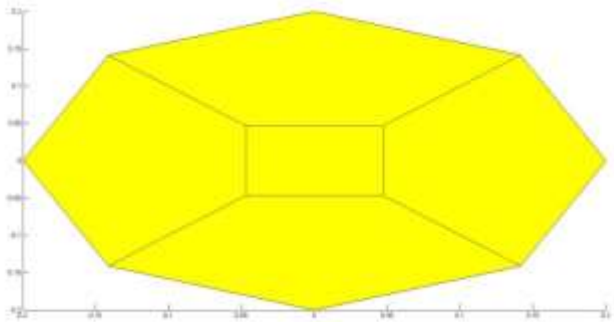

Fig.4.1.3a Showing Top Surface of Right Circular Cylinder

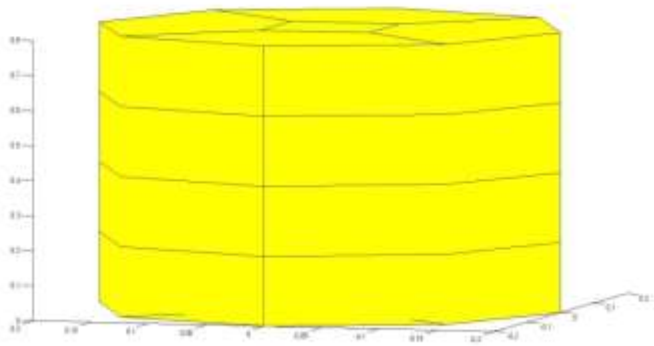

Fig.4.1.3b Right Circular Cylinder

The radius of the Right Circular Cylinder is taken as 0.2m and its length as 0.8m (4.1.3a). The top and face of the cylinder is divided into 5 numbers of elements whereas laterally it is divided into 16 numbers of elements. As a whole, it is divided into 16 numbers of elements and a total of 80 numbers of nodes. The CHIEF is taken in the mid-point of the cylinder.

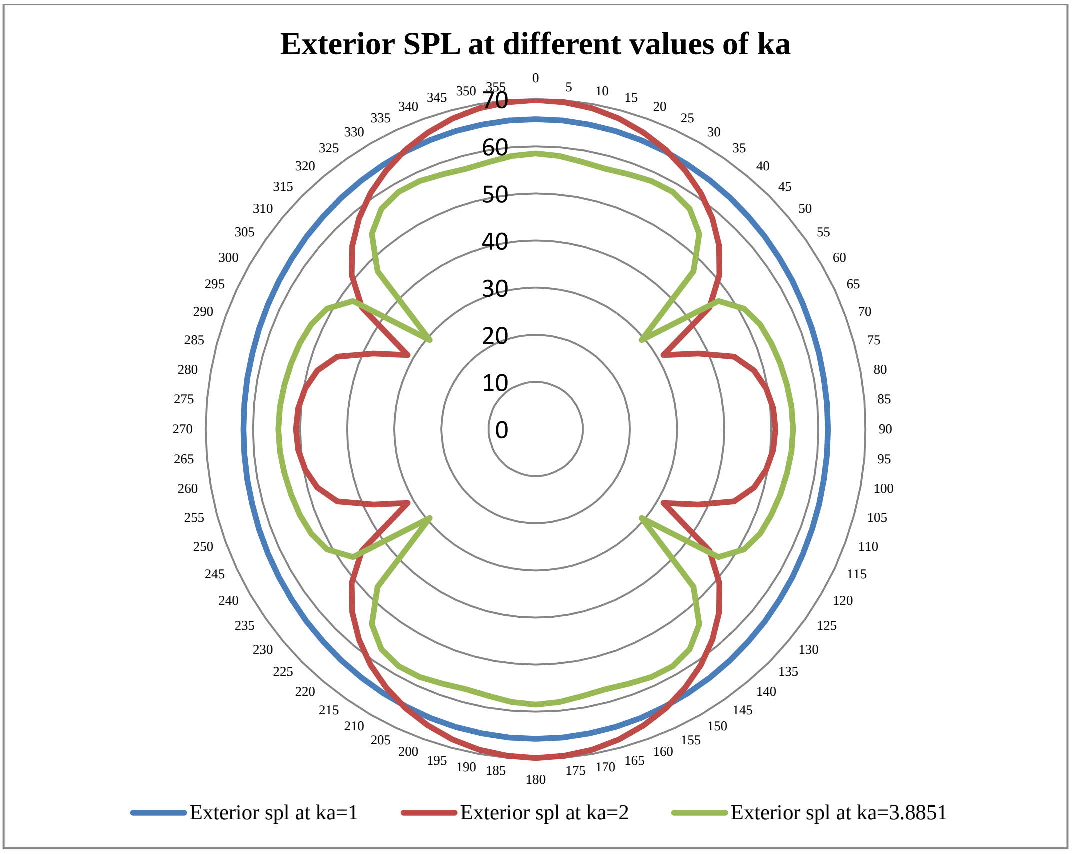

Fig.4.1.3c Far field pressure of a Cylinder

Figure (4.1.3c) shows the far field pressure pattern of a cylinder of radius *a* (=0.2m) and of length *4a* (=0.8m), where the pressure is plotted against polar angle taken at distance of 2m (10a = 10*0.2) from the centre of the right circular cylinder for ka = 1, 2 and 3.8851[15, 46]. For ka=1, the farfield pressure is nearly uniform. But for *ka*=2 and 3.8851, it is showing huge change in sound pressure level in dB with change in angle.

4.2 INTERIOR ACOUSTICS

Five case studies are shown in this part as follows.

- **a)** Case study of rigid rectangular cavity of two different sizes
- **b)** Case study of three rigid arbitrary shaped cavity

4.2.1 CASE STUDY OF A RECTANGULAR CAVITY OF 1.8M LENGTH

A rigid container of dimension 1.8m x 0.6m x 0.6m is taken in this problem (Fig. 4.2.1a). The air inside acts as an interior acoustic domain. The rectangular cavity had been divided into 126 elements having a total of 274 numbers of nodes. The pulsating face (left face) as well as right face are divided into 9 elements.

The speed of sound, c, is taken to be 340m/s and the density of air, ρ, is 1.20 kg/m^3. The medium is excited by a sinusoidal motion of the left wall, acting as a rigid piston, with velocity amplitude of 0.001m/s. The responses are calculated at a forcing frequency interval of 10 radian/s. Fig. 4.2.1c and 4.2.1d show the sound pressure level (SPL) in decibels (dB) (with a threshold pressure of 2×10^{-5} N/m^2), computed analytically and by using boundary element method at the midpoint of the right wall, and also at the centre of the domain. The analytical solutions and numerical results show very close conformity. Analytically, the acoustic resonance at the right boundary is scheduled to occur when $\Omega = nc\pi / L$, where L is the length of the duct, whereas, at the centre of the domain, the resonance takes place at $\Omega = 2nc\pi / L$. For the present purpose, analytically, the resonance at the right side boundary should occur at frequencies of 0, 593.412, 1186.824… radian/s while, that occurs at the centre of the domain at 0, 1186.824, 2373.648…radian/s by putting the value of n as 0,1,2 like so on and length as 1.8m. This is evidently being observed in the BE solution.

This cavity is analysed using absorbent layer also. 30 mm thick polyurethane foam sheets is applied as absorbent layers [29]. Comparison was shown for the following cases.

Four cases are done under this case study.

i. No absorbent layer at any face of the cavity
ii. Absorbent layer provided at the top face of the cavity
iii. Absorbent layer provided at the rightmost wall
iv. Absorbent layer provided at the front and back wall

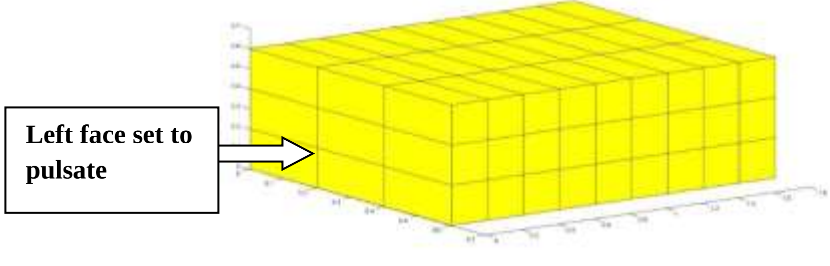

Fig.4.2.1a Showing left face (Pulsating face) of Rectangular cavity of 1.8m length

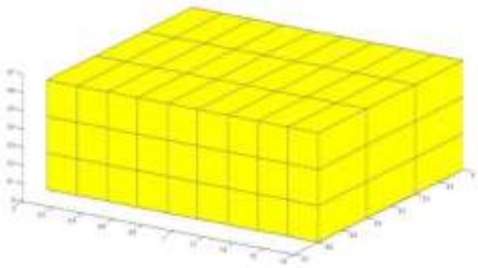

Fig.4.2.1b Showing Right face of Rectangular cavity of 1.8m length

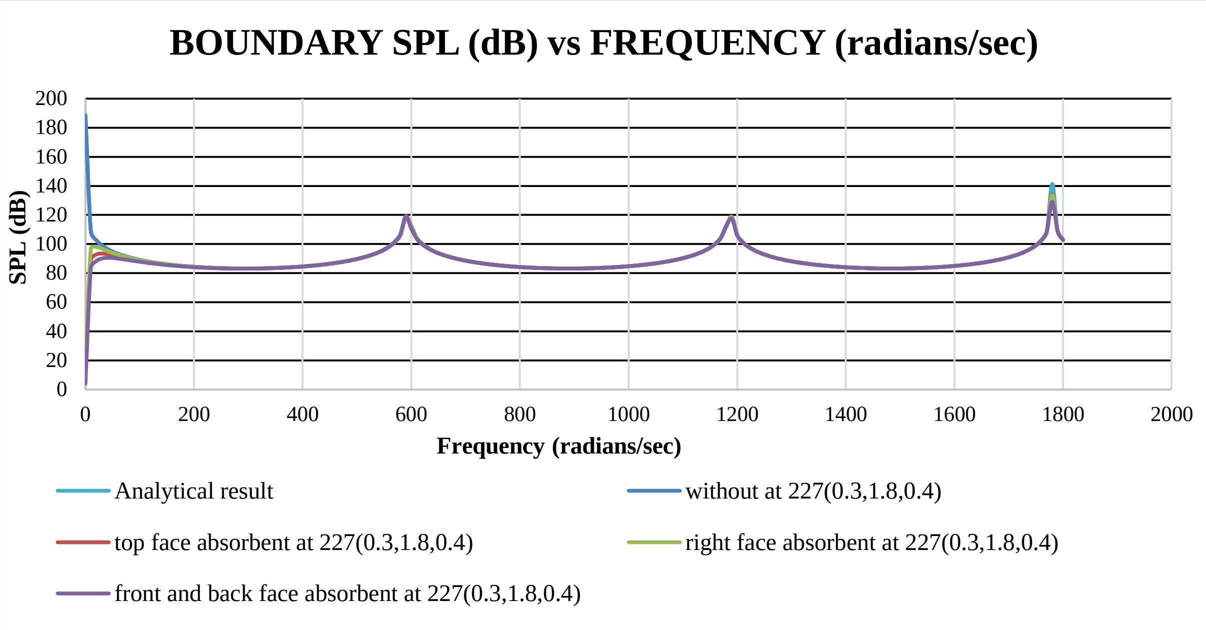

Fig.4.2.1c Boundary SPL for different cases of absorbent layer

The first peak can be observed at 593.001 radians/sec whereas other peaks can be observed at 1187.001 radians/sec, 1781.001 radians/sec respectively. For the first peak SPL, for the four different cases are 136.21dB, 120.18dB, 122.26dB and 117.8Db respectively. At 1187.001 radians/sec, the SPL for four different cases are 147.62dB, 136.89dB, 139.35dB and 132.03dB respectively. For the above two peaks SPL for providing absorbent layer at the front and back face is least among all the cases. Last but not the least for third peak absorbent layer at the front and back face is least as well. The resonating frequencies i.e. the peaks matches with the analytical results.

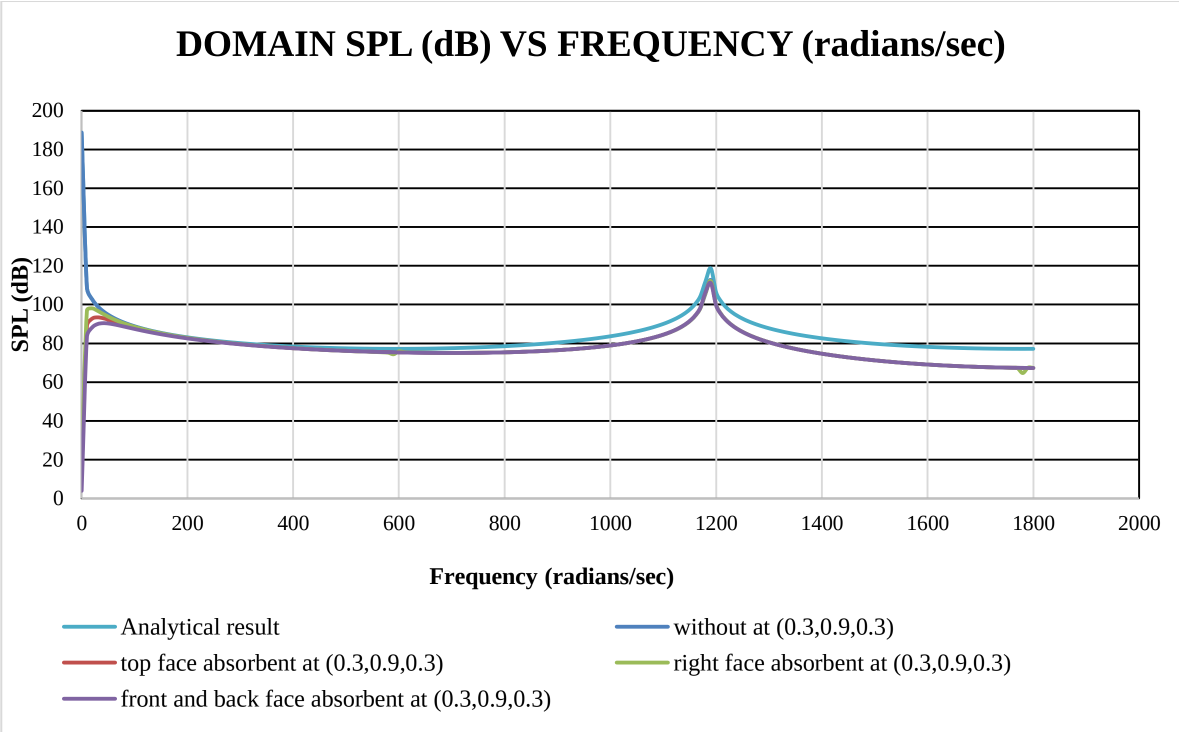

Fig.4.2.1d Domain SPL for different cases of absorbent layer

In case of Domain SPL the resonating frequency occur at 1187.001 radians/sec. The SPL values for the four cases are 141.32dB, 130.59dB, 133.05dB and 125.73dB respectively. It can be observed that the SPL for Boundary as well as Domain is least in case of having absorbent layer at front and back face of the cavity.

4.2.2 CASE STUDY OF A RECTANGULAR CAVITY OF 1.2M LENGTH

In this case the cavity size is reduced to 1.2m (Fig.4). The cross-section is rectangular with each side 0.6m. The arbitrary cavity had been divided into 90 elements having a total of 272 numbers of nodes. The pulsating face (left face) as well as the right face is divided into 9 numbers of elements.

The left hand wall is set to execute simple harmonic motion where the velocity amplitude is set at 0.001 m/s. The forcing frequency is limited to 1800 rad/s computed at an interval of 10 rad/s. The sound pressure level at the mid-point of right vertical plane (0.4, 1.2, 0.3) and at the domain (0.3, 0.6, 0.3) was found out numerically. Absorbent layers are provided at the faces of the cavity and the result is compared in Fig. 4.2.2b and 4.2.2c.

Four cases are done under this case study.

i. No absorbent layer at any face of the cavity
ii. Absorbent layer provided at the top face of the cavity
iii. Absorbent layer provided at the rightmost wall
iv. Absorbent layer provided at the front and back wall

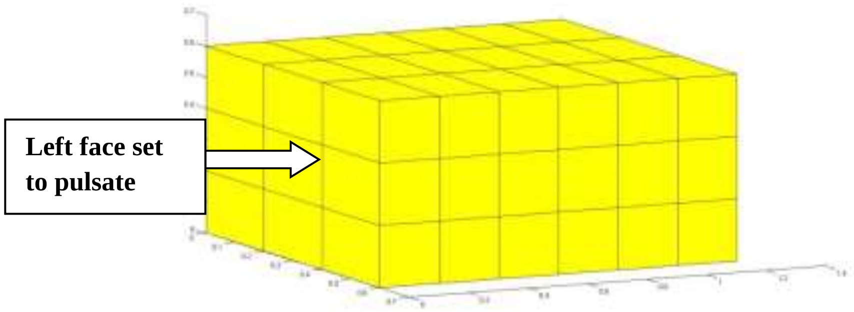

Fig.4.2.2a Rectangular cavity of 1.2m length

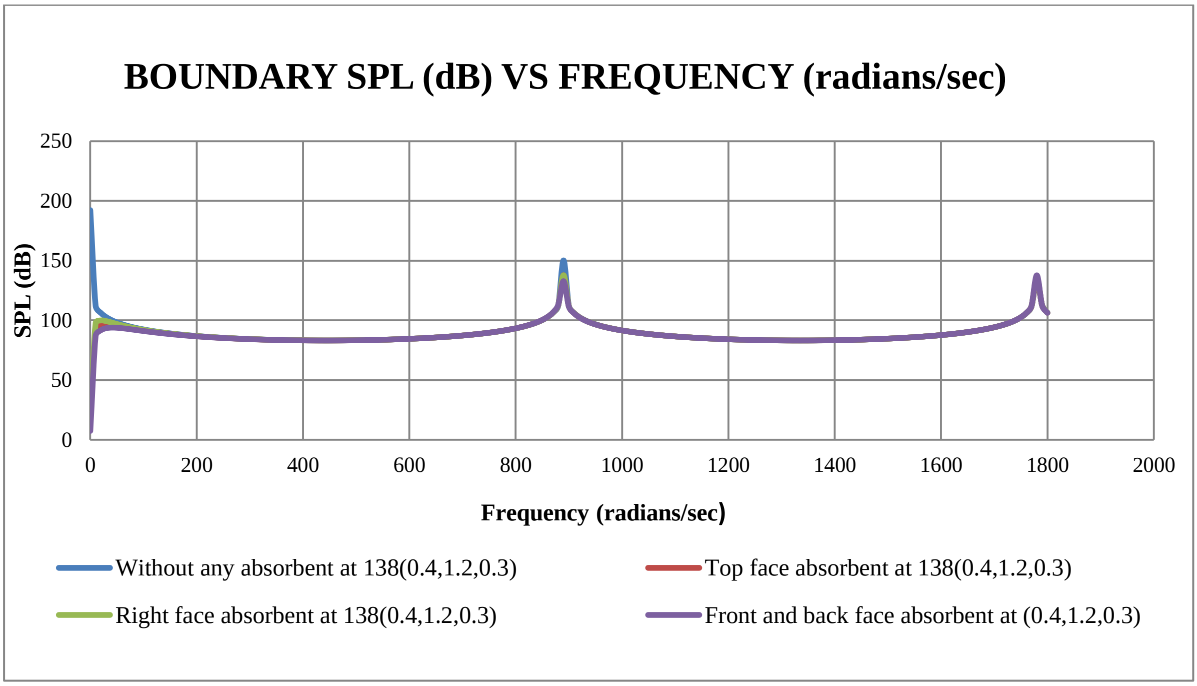

Fig4.2.2b Boundary SPL for different cases of absorbent layer

The first peak can be observed at 890.001 radians/sec whereas other peak can be observed at 1780.001. For the first peak the SPL, for the four different cases are 150.17dB, 137.74dB, 137.75dB and 132.81dB respectively. It can be said that at first resonating frequency the SPL is least when absorbent layer is provided at front and back face of the cavity. At the second peak benefit of using absorbent layer is not seen both at boundary and domain.

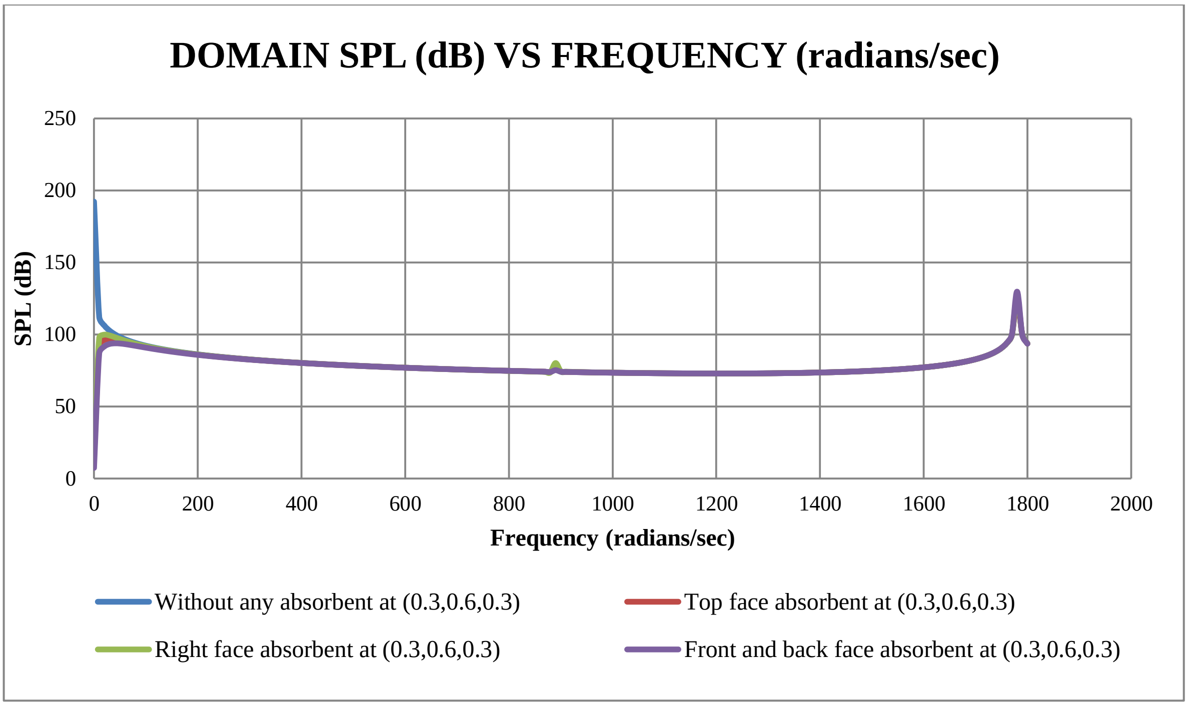

Fig4.2.2c Domain SPL for different cases of absorbent layer

4.2.3 CASE STUDY OF ARBITRARY SHAPED RIGID CAVITY 1

A rectangular cavity with one inclined plane as shown in Fig.4.2.3a and 4.2.3b had been used. The bottom length of the cavity is 1.8m and the top length is 1.6m. The cross-section is rectangular with each side 0.6m. The arbitrary cavity had been divided into 72 elements having a total of 218 number of nodes. The pulsating face (left face) as well as right face are divided into 4 number of elements. The left hand wall is set to execute simple harmonic motion where the velocity amplitude is set at 0.001 m/s. The forcing frequency is limited to 1800 rad/s computed at an interval of 10 rad/s. The sound pressure level at the mid-point of inclined plane (0.3, 1.7, 0.3) and at the domain (0.3, 0.9, 0.3) was found out numerically. Absorbent layers are provided at the faces of the cavity and the SPL value is compared for the following cases.

Four cases are done.

i. No absorbent layer at any face of the cavity
ii. Absorbent layer provided at the rightmost wall
iii. Absorbent layer provided at the top face of the cavity
iv. Absorbent layer provided at the front and back wall

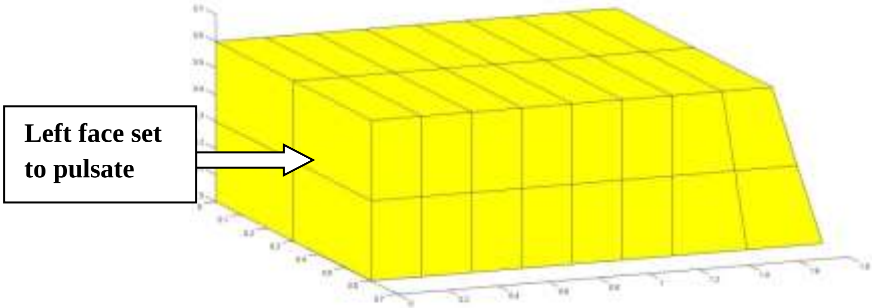

Fig.4.2.3a Showing left face (Pulsating face) of arbitrary cavity

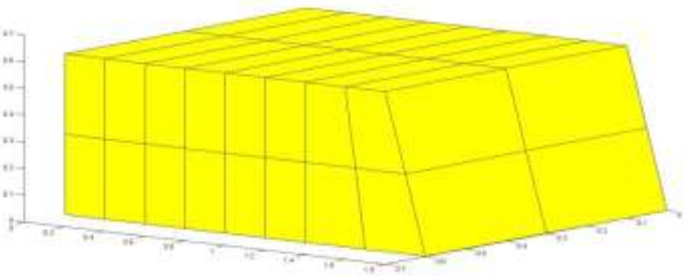

Fig.4.2.3b Showing Right face of arbitrary cavity

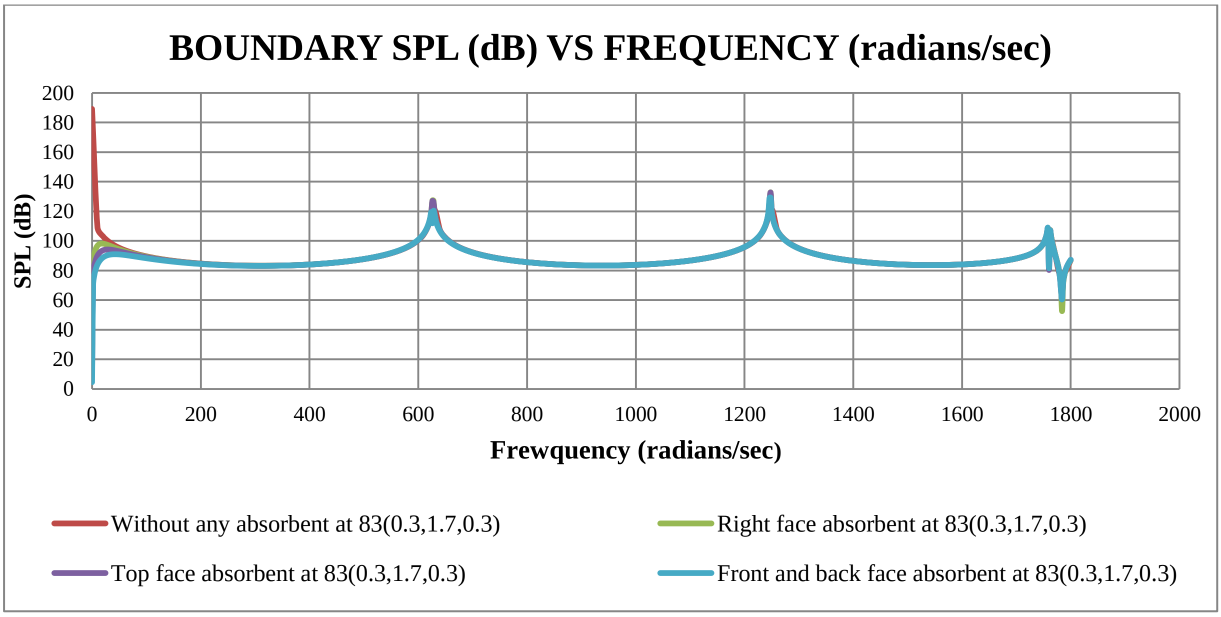

Fig4.2.3c Boundary SPL for different cases of absorbent layer

It is observed that the peaks are visible at 628 radian/s and 1248 radian/s. At both peaks, it is clear that addition of absorbent layer reduces SPL to some extent. For example, at 628 rad/s the SPL in dB for case i, ii, iii and iv are 134.1, 127.2, 126.3 and 120.2 respectively. Whereas at 1248 radian/s, the SPL values are 136.2, 132.6, 132.8 and 129.2. The position of absorbent layer plays a very important role in reducing the SPL. In the present case when absorbent layer is provided at front and back of the cavity, the reduction in SPL is maximum. Also the effect of absorbent layer is prominent in the first peak region. It is also observed that the absorbent layer only plays its role at the resonant points.

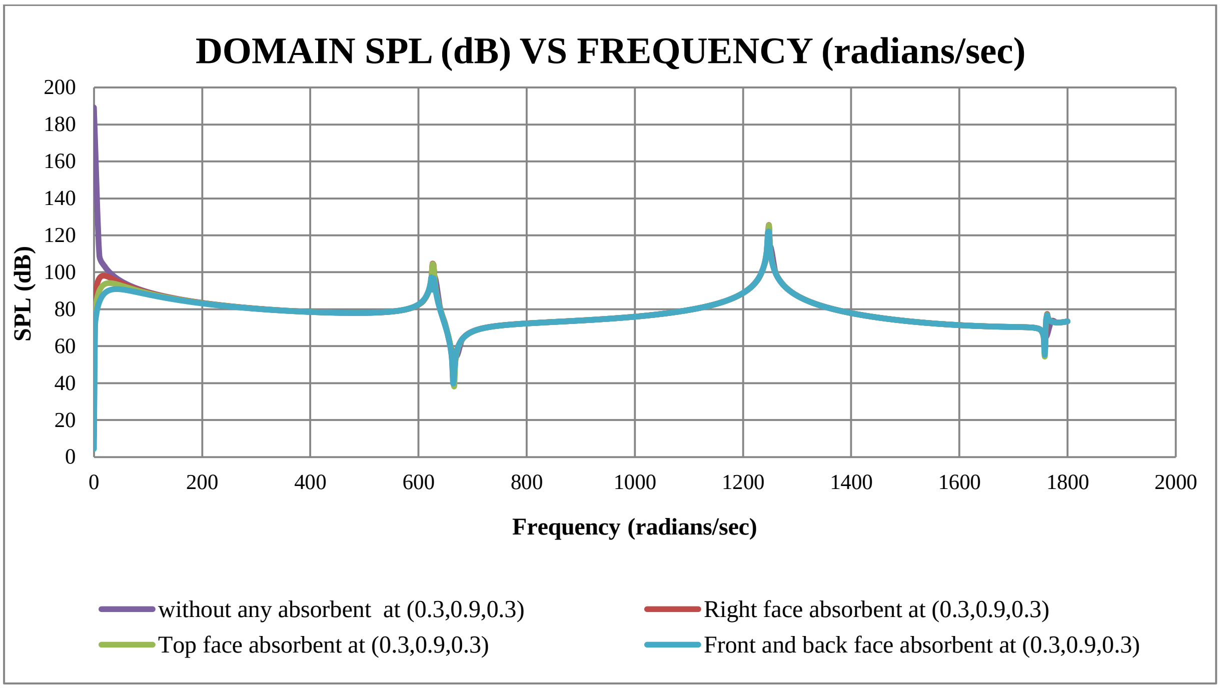

Fig4.2.3d Domain SPL for different cases of absorbent layer

From Fig. 4.2.3d, the peak can be observed at 1248 radian/sec but this graph is different from the graph of Domain SPL in case of rectangular cavity. At 628 radians/sec there is abrupt change in SPL can be seen where the first peak for Boundary SPL has occurred. At 1248radian/s the values are 129.0dB, 125.50dB, 125.36dB and 121.9dB respectively. It is observed that absorbent layer at the front and back face is more beneficial than other cases.

4.2.4 CASE STUDY OF ARBITRARY SHAPED RIGID CAVITY 2

In this study, an arbitrary shaped cavity as shown in Fig.4.2.4a and 4.2.4b had been used for interior acoustic problem for calculating sound pressure level (SPL) at the boundary as well as at the domain using boundary element analysis (BEA). The bottom length of the cavity is 1.8m and the top length is 1.2m. The cross-section is rectangular with each side 0.8m maintained till 1.2m of its length. The arbitrary cavity had been divided into 88 elements having a total of 280 numbers of nodes. The pulsating face (Right vertical face) is divided into 4 numbers of elements. The right hand vertical wall is set to execute simple harmonic

motion where the velocity amplitude is set at 0.001 m/s. The forcing frequency is limited to 1500 rad/s computed at an interval of 10 rad/s. The sound pressure level at the mid-point of left vertical plane (0.4,0,0.4) and at the domain (0.3,0.9,0.3) was found out numerically and compared for different cases in Fig. 4.2.4c and 4.2.4d.
Four cases are done.

i. No absorbent layer at any face of the cavity
ii. Absorbent layer provided at the leftmost vertical wall
iii. Absorbent layer provided at the top face of the cavity
iv. Absorbent layer provided at the front and back wall

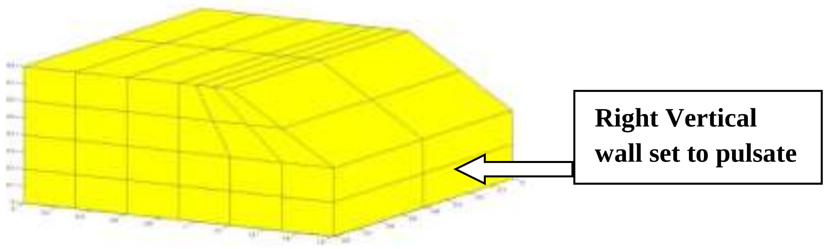

Fig.4.2.4a Showing right face (Pulsating face) of arbitrary cavity

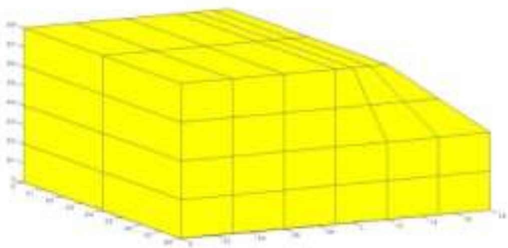

Fig.4.2.4b Showing left face of Arbitary cavity

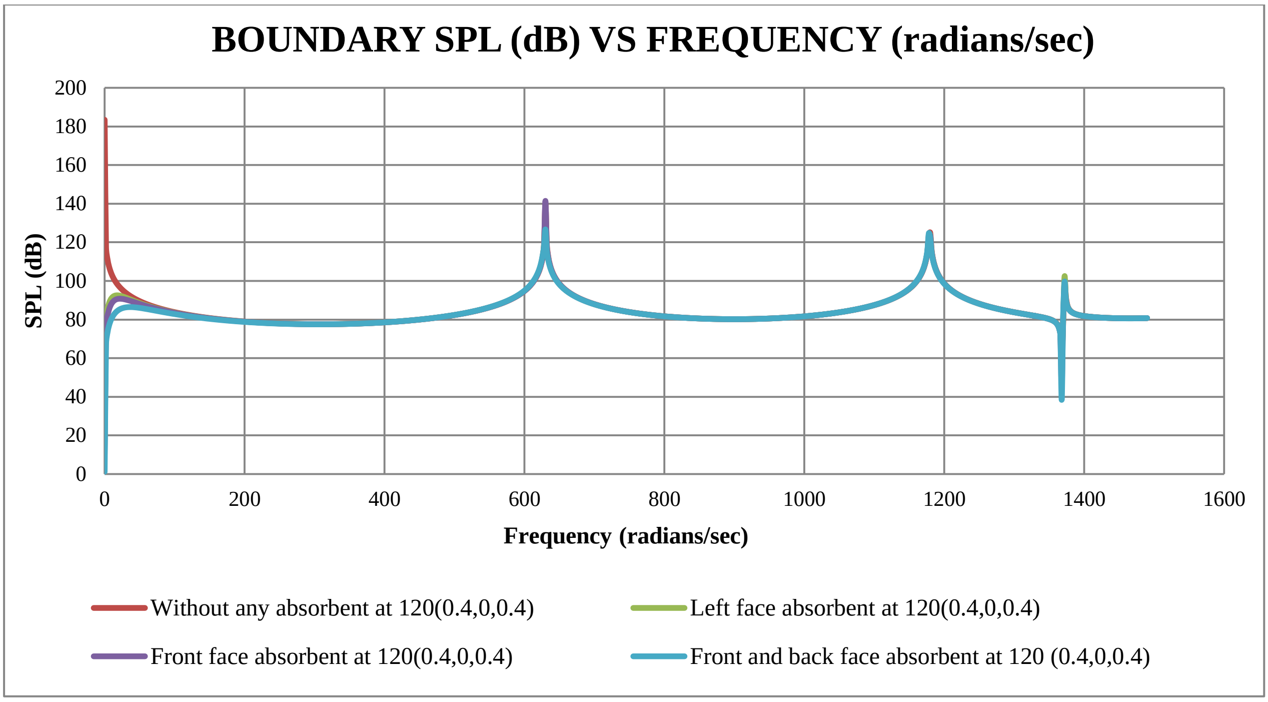

Fig4.2.4c Boundary SPL for different cases of absorbent layer

It is seen that that use of absorbent layer reduces SPL to a great extent at resonant points i.e., 630 rad/s and 1180 rad/s, when these are provided at front and back of the cavity. At 630rad/s the SPL values for the above four cases are140.1dB, 135.61dB, 141.45 dB and 126.68 dB. But surprisingly no benefit is seen when absorbent layer is provided at top of the cavity for 630 rad/s. At 1180 radians/s the SPL are 125.01 dB, 123.85 dB, 123.63 dB and 122.13 dB respectively. The percentage reduction in SPL is very less at higher forcing frequency.

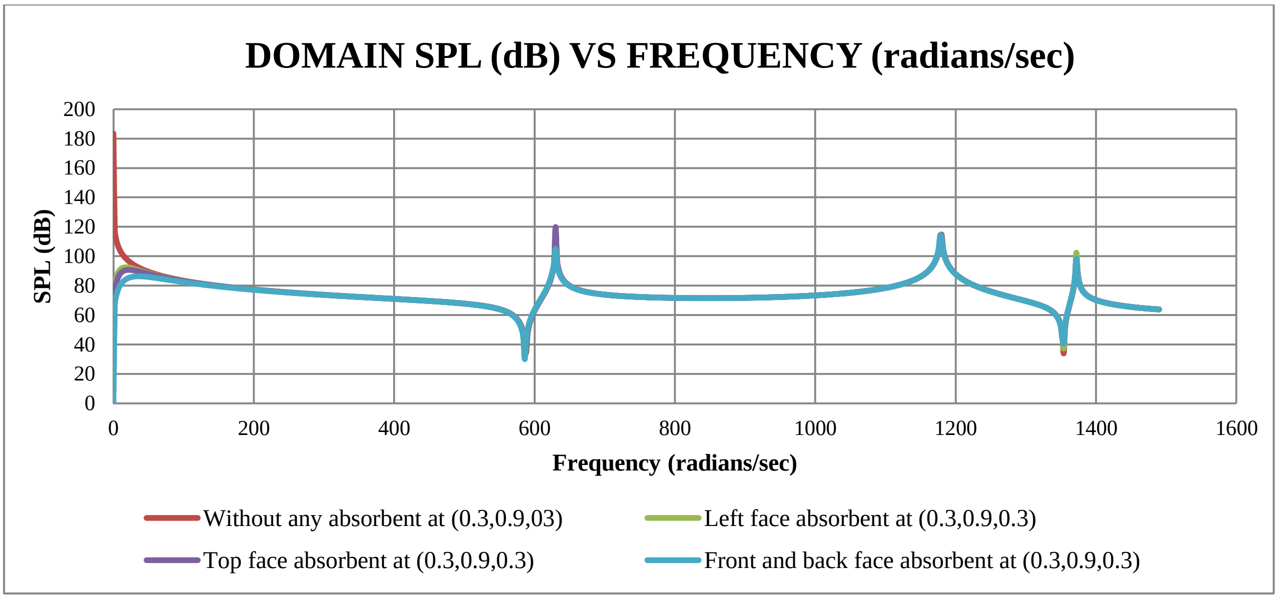

Fig4.2.4d Domain SPL for different cases of absorbent layer

In domain SPL graph (Fig. 4.2.4d) at 630 radians/sec there is abrupt change in SPL can be seen where the first peak for Boundary SPL has occurred. At 1180 radian/s the values are 114.65dB, 113.50dB, 113.26dB and 111.80dB respectively. It is observed that absorbent layer at the front and back face is more beneficial than other cases at the first resonant point.

4.2.5 CASE STUDY OF ARBITRARY SHAPED RIGID CAVITY 3

An arbitrary shaped cavity as shown in Fig.4.2.5a and 4.2.5b had been used for interior acoustic problem for calculating sound pressure level (SPL) at the boundary as well as at the domain using boundary element analysis (BEA). The bottom length of the cavity is 2m and the top length is 0.8m having two inclined faces coming down from its top face till its middle height in symmetrical manner. The cavity had been divided into 64 elements having a total of 194 number of nodes. The pulsating face (right face) is divided into 4 number of elements. The right hand vertical wall is set to execute simple harmonic motion where the velocity amplitude is set at 0.001 m/s. The forcing frequency is limited to 1800 rad/s computed at an interval of 10 rad/s. The sound pressure level at the mid-point of left vertical plane (0.4,0,0.2) and at the domain (0.4,1.0,0.4) was found out numerically with and without using absorbent layers for the following cases and the result is compared in Fig 4.2.5c and 4.2.5d.

i. No absorbent layer at any face of the cavity
ii. Absorbent layer provided at the top face of the cavity
iii. Absorbent layer provided at the leftmost vertical as well as the inclined wall
iv. Absorbent layer provided at the front and back wall

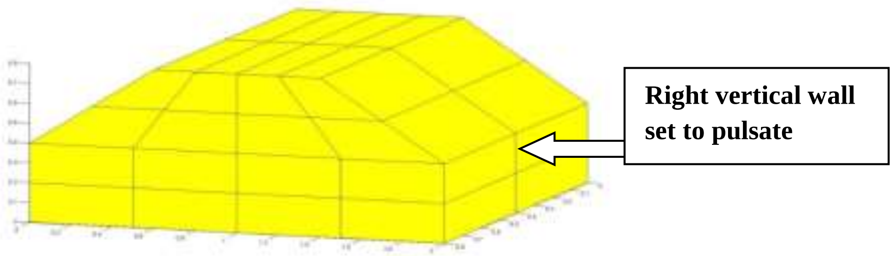

Fig.4.2.5a Showing right face (Pulsating face) of arbitrary cavity

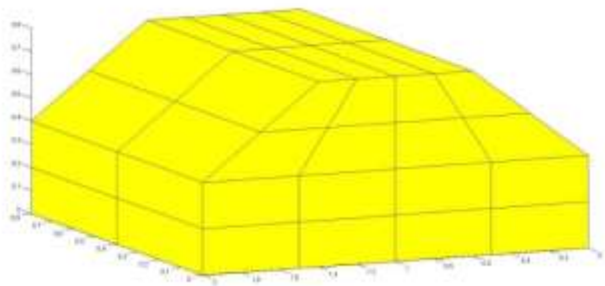

Fig.4.2.5b Showing left face of arbitrary cavity

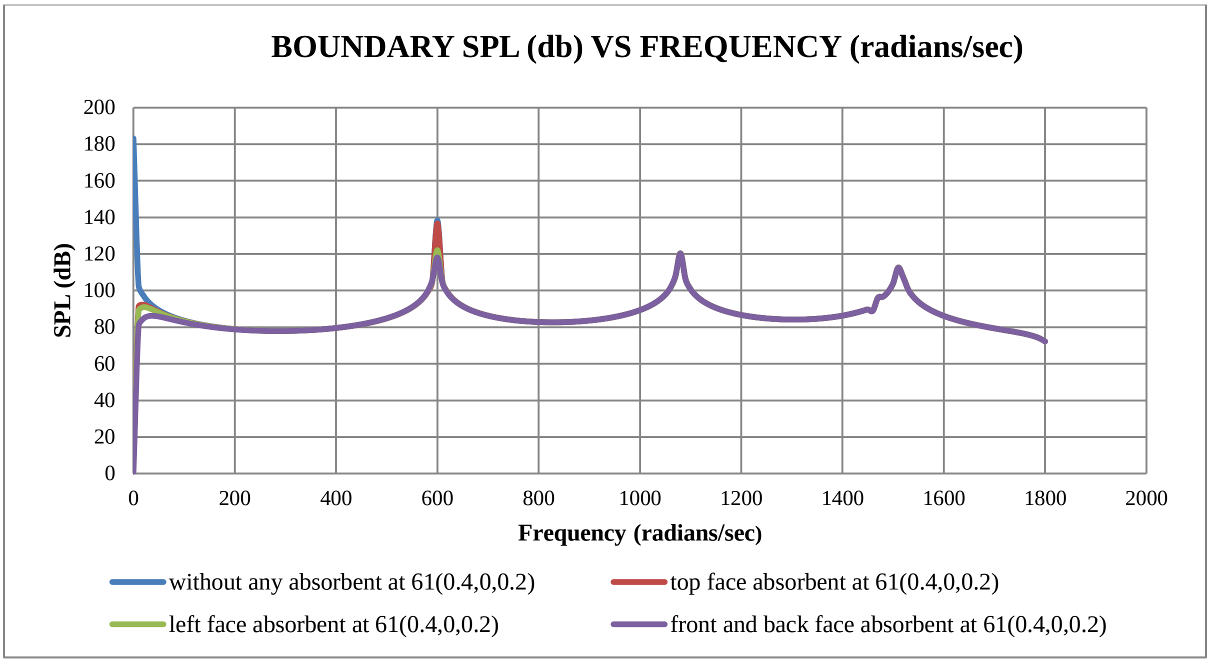

Fig4.2.5c Boundary SPL for different cases of absorbent layer

The first peak can be observed at 600.001 radians/sec whereas other peaks can be observed at 1080.001, 1510.001 respectively. For the first peak, sound pressure level four different cases are 138.37 dB, 136.76 dB, 122.11 dB and 118.08 dB respectively. At 1080.001 radians/sec the SPL, for four different cases are 120.03 dB, 120.43 dB, 120.46 dB and 120.31 dB respectively. For 1510.001 radians/sec the SPL, for four different cases are 112.64 dB, 112.58 dB, 120.53 dB and 112.44 dB respectively. It can be seen that for first resonating frequency the SPL is least when absorbent layer is provided in the front and back. For the second resonating frequency there is no such decrease in SPL by providing absorbent layer in any of the face of the arbitrary cavity. In case of third resonating frequency there is very less decrement in SPL when absorbent layer is provided in the front and back face.

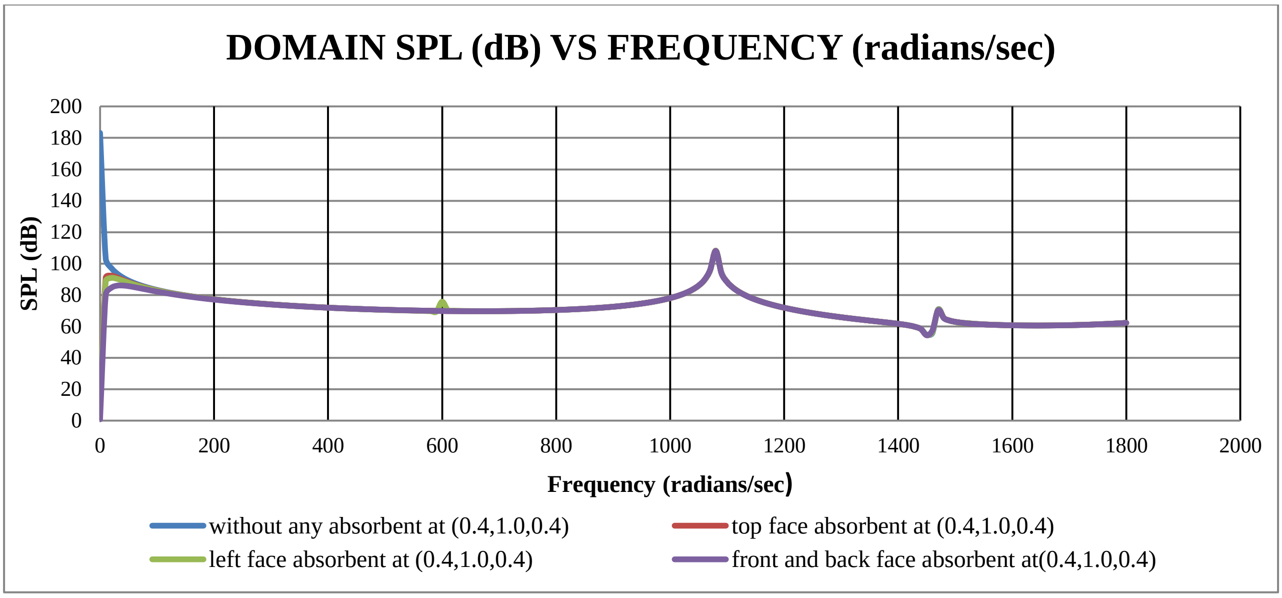

Fig4.2.5d Domain SPL for different cases of absorbent layer

In case of Domain SPL the resonating frequency occur at 1080.001 radians/sec. The SPL values for the four cases are 107.80 dB, 108.20 dB, 108.24 dB and 108.10 dB respectively. It can be observed that by providing absorbent layer in any face of the arbitrary cavity no decrease in SPL can be seen at this frequency.

5. CONCLUSION

The noise produces irritation and causes various health problems. Reduction of excessive noise is only possible through proper prediction and control of excessive noise only. In this present thesis a numerical study has been performed to predict and regulate high sound pressure level. Boundary element method has been adopted to solve the acoustic problem. The benefits of using boundary element method (BEM) over other domain methods are that only boundary of the problem domain need to be modelled, thus reducing computation time and storage. A MATLAB program has been developed. Both exterior and interior acoustic analysis have been done.

In the **exterior analysis**, the radiation of acoustic wave from arbitrary shaped body submerged in air has been analysed using BEM. The sound pressure level is evaluated on the surface and at a point far from the body has been found out. Though the domain is infinite in this case, only surface of the arbitrary shaped body has been discretized. But there is shortcoming of this method too. The major disadvantage of integral equation method is the well-known failure of certain integral equation when applied to exterior problem to yield unique solution at the characteristic values of wave number.
To overcome this non-uniqueness problem the Combined Helmholtz Integral Equation Formulation (CHIEF) method originally proposed by Schenck [15] has been applied. One CHIEF point is applied at the centre of the body and it was shown to work well for the monopole problem.

This program firstly finds the surface pressure on the arbitrary shaped body i.e., cube and cylinder and then the far field pressure at the domain has been found out. It was shown that with change in angle, the sound pressure level changes at a distance.

In the **interior analysis,** the same boundary element code has been used. There are only two differences that need to be checked in the interior analysis. The normal directions are opposite to each other and the solid angles are different at corners and edges.
Our BEM code is validated with the analytical solution for a duct problem. It was shown that the sound pressure level at the boundary and at the centre of the domain matches well with analytical solution. In this thesis the effect of using absorbent layer on the inner faces of the boundaries of the acoustic cavity is shown and compared. The shape of the cavity has been changed. Almost for all the cases, addition of the absorbent layer reduces the SPL at the first resonance point. The reduction effect almost nil at higher frequency. Also position of absorbent layer plays a very important role. When the absorbent layer is placed at front and back wall it works best.
It is found that the absorbent inflicts an additional kink in the acoustic pressure curve for a point inside the domain in between two consecutive peaks. This kink is very much prominent in un-symmetrical cavity as in case 4.2.3 and 4.2.4.

Thus, proper investigation and finally a prototype testing are essential for effective noise and vibration control. At the same time the knowledge of the operating frequency band is also essential. With every possible available data at hand, trials could be undertaken to control the sound pressure levels to bring them within specified limits.

6. REFERENCES

[1] Green, G (1828) An Essay on the Application on Mathematical Analysis to the Theories of Electricity and Magnetism, Notingham.

[2] Betti, E (1872) Theoria dell’ Elasticia, il Nuovo Cimento, Ser. 2, pp.7-10.

[3] Somigliana, C (1885) Sopra l’ Equilibrio di’ un Corpo Elastico Isotropo, Il Nuovo Comento, Ser. 3, pp. 17-20.

[4] Trevelyan, J (1993) Applications of the BEASY Boundary Element Software in Engineering Industry, in: Aliabadi, M.H. (ed.), Industrial Applications of the Boundary Element Method, Computational Mechanics Publications, Southampton.

[5] Beskos, D.E (1987) Boundary Element Methods in Dynamic Analysis. Part I, Applied Mechanics Reviews, Vol.40, pp. 1-23.

[6] Beskos, D.E (1997) Boundary Element Methods in Dynamic Analysis. Part II, Applied Mechanics Reviews, Vol.50, pp. 149-197

[7] Encarnacao, J., and Schlechtendahl, J. (1983) Computer Aided Design. Springer Verlag, Berlin.

[8] Deist, F.H. and Georgiadis, E (1973) A computer system for three-dimensional stress analysis in elastic media. Rock Mechanics 5: 189-202.

[9] Ergatoudis, J.G., Irons, B.M. and Zienkiewicz O.C (1968) Three dimensional analysis of arch dams and their foundations. Proc. Symp. Arch Dams. Inst. Civ. Eng.

[10] Lachat, J.C and Watson J.O (1991) Introduction to finite and Boundary Element Methods for Engineers. J.Wiley.

[11] Chen, L.H. and Schwikert, D.G (1963) Sound Radiation from an Arbitrary body. Journal Of the Acoustical Society of America, Vol. 35, No. 10, pp. 1626-1632.

[12] Chertock, G (1964) Sound Radiation from Vibrating Surfaces. Journal of the Acoustical Society of America, Vol. 36, No. 7, pp. 1305-1313.

[13] Williams, W, et al (1964) Acoustic Radiation from a Finite Cylinder. Journal of the Acoustical Society of America, Vol. 36, No. 12, pp. 2316-2322.

[14] Copley, L.G (1967) Integral Equation Method for Radiation from Vibrating Bodies. Journal of the Acoustical Society of America, Vol. 41, No. 4, pp. 807-816.

[15] Schenck, H.A (1968) Improved Integral Formulation for Acoustic Radiation Problems. Journal of the Acoustical Society of America, Vol. 44, No. 1, pp. 41-58.

[16] Meyer, W.l., Bell. W.A., and Zinn, B.T (1978) Boundary Integral Solutions of Three Dimensional Acoustic Radiation Problems. Journal of Sound and Vibration, Vol. 59, No. 2, pp. 245-262.

[17] Koopman, G.H., and Benner, H (1982) Method for computing the Sound Power of Machines Based on the Helmholtz Integral. Journal of the Acoustical Society of America, Vol. 71, No. 1, pp. 78-89.

[18] Seybert, A.F., et al (1983) Application of the BIE Method to Sound Radiation Problems Using an Isoparametric Element. ASME paper No. 82-WA/NCA-1.

[19] Piaszczyk, C.M (1984) Acoustic Radiation from Vibrating Surfaces at Characteristic Frequencies. Journal of the Acoustical Society of America, Vol. 75, No. 2, pp. 363-375.
[20] Brod, K (1984) On the Uniqueness of Solution for all Wavenumbers in Acoustic Radiation. Journal of the Acoustical Society of America, Vol. 76, No. 4, pp. 1238-1243.
[21] Wu, T.W., et al (1990) Vectorization and Parallelization of the Acoustic Boundary Element Code BEMAP on the IBM ES/3090 VF. International Congress on Recent Developments in Air-and Structure-Borne Sound and Vibration, Auburn University, USA.
[22] Seybert, A.F., Cheng, C.Y., and Wu, T.W (1990) The solution of Coupled Interior/Exterior Acoustic Problems Using the Boundary Element Method. Journal of the Acoustical Society of America, Vol. 88, No. 3, pp. 1612-1618.
[23] Bell, W.A., Meyer, W.L., and Zinn, B.T (1977) Predicting the Acoustics of Arbitrarily Shaped Bodies Using an Integral Approach. AIAA Journal, Vol. 15, No. 6, pp. 813-820.
[24] Dowell, E.H (1980) Master plan for Prediction of Vehicle Interior Noise. AIAA Journal, Vol. 18, No. 4, pp. 353-366.
[25] Sestieri, A., Vescovo, D.D., and Lucibello, P (1984) Structural-Acoustic Coupling in complex Shaped Cavities. Journal of the Sound and Vibration, Vol. 96, No. 2, pp. 219-233
[26] Seybert, A.F., Cheng, C.Y.R (1987) Application of the BEM to Acoustic Cavity Response and Muffler Analysis. J. Vib. Ac. St. Rel. Des., Vol. 109, pp. 15-21.
[27] Fyfe, K.R (1988) Determination of Acoustic Modal Properties from Boundary Element Modeling. Dynamic Engng., Heverlee, Belgium.
[28] Cheng, C.Y.R., and Seybert, A.F (1988) Recent Applications of the Boundary Element Method to Problems in Acoustics. SAE Paper No. 870997, pp. 3.165-3.174.
[29] Suzuki, S., Maruyama, d., and Ido, H (1989) Boundary Element Analysis of Cavity Noise Problems with Complicated Boundary Conditions. Journal of the Sound and Vibration, Vol. 130, No. 1, pp. 79-91
[30] Ishiyama, S.I., et al (1989) The Applications of ACOUST/BOOM-A Noise Level Predicting and Reducing Computer Code. SAE Transactions Paper, pp. 4.976-4.986.
[31] Niyogi, A.G (2006) Structural Acoustic Problems with Absorbent Layers Within Laminated Composite Enclosures. J. Vib. Acoust 128(6) 705-712.
[32] Ning, Han, Cheuk MingMak (2009) Prediction of the absorption component in rectangular enclosures with a single absorbent boundary. Applied Acoustics, Vol. 70, Issue 2, pp. 297-299.
[33] Kinsler, L.E., Frey, A.R., Coppens, A.B., and Sanders, J.V (1982) Fundamentals of Acoustics, 3rd Ed., John Wiley & Sons, Chichester.
[34] Brebbia, C.A (1978) The Boundary Element Method for Engineers. Pentech Press, London.
[35] Seybert, A.F., T.W Wu, W.L. Li (1990) Applications of the FEM and BEM in structural acoustics, in Tanaka, M., Brebbia, C.a., Honma, T., (Eds.) Boundary Elements Be XII, Vol.-2, Applications in Fluid Mechanics and Field Problems, CMP-Springer, Verlag, pp. 171-182.

[36] Kupradze VD (1956) Boundary value problems in vibrational theory and integral equations. Deutscher Verlag der Wissenschaften, Berlin (1st Russian edition 1950)
[37] Weyl H (1952) Kapazitat von Strahlungsfeldern. Mathematishe Zeitschrift 55: 187-198
[38] Wu TW, Seybert AF (1991) Acoustic radiation and scattering. Chapter 3 of [6] 61 – 76
[39] Wu TW, Seybert AF (1991) A weighted residual formulation for the CHIEF method in acoustics. Journal of the Acoustical Society of America 90: 1608-1614
[40] Wu TW (1994) The Helmholtz integral equation. Chapter 2 of [45] 9-28
[41] Schenck HA (1968) Improved integral formulation for acoustic radiation problems. Journal of the Acoustical Society of America 44:41-58
[42] Panic OI (1965) K voprosu o razresimosti vnesnich kraevich dlja volnovogo uravnenija I dlja sistemi uravnenij MAXWELLa. Uspechi Mathematickich Nauk 20:221-226
[43] Brakhage H, Werner P (1965) Uber das Dirichlet'sche Aubenraumproblem fur die Helmholtz'sche Schwingungsgleichung. Archiv der Mathematik 16:325-329
[44] Burton AJ, Miller GF (1971) The application of integral equation methods to the numerical solution of some exterior boundary-value problems. Proceedings of the Royal Society of London 323:201-220
[45] Computation Acoustics of Noise Propagation in Fluids - Finite and Boundary Element Methods. Chapter 15 – Treating the phenomenon of Irregular Frequencies.
[46] A.F. Seybert, B. Soenarko, F.J. Rizzo, and D. J. Shippy (1984) An advanced computational method for radiation and scattering of acoustic waves in three dimensions.